frontiers | Frontiers in Astronomy and Space Sciences

TYPE Original Research
PUBLISHED 30 October 2023
DOI 10.3389/fspas.2023.1186173

OPEN ACCESS

EDITED BY
Fulvio Franchi,
Botswana International University of Science and Technology, Botswana

REVIEWED BY
Nicolas Mangold,
UMR6112 Laboratoire de Planetologie et Geodynamique (LPG), France
Aaron Cavosie,
Curtin University, Australia

*CORRESPONDENCE
Philippe Lambert,
lambertbdx@gmail.com

†These authors have contributed equally to this work

RECEIVED 14 March 2023
ACCEPTED 06 September 2023
PUBLISHED 30 October 2023

CITATION
Lambert P and Reimold WU (2023), Terrestrial impact sites as field analogs for planetary exploration.
Front. Astron. Space Sci. 10:1186173.
doi: 10.3389/fspas.2023.1186173

Terrestrial impact sites as field analogs for planetary exploration

Philippe Lambert[1]*† and Wolf Uwe Reimold[2]†

[1]CIRIR–Center for International Research and Restitution on Impacts and on Rochechouart, Rochechouart, France, [2]Laboratory of Geochronology and Isotope Geology, Institute of Geosciences, Postgraduate Program in Geology, University of Brasília, Brasília, Brazil

Terrestrial impact structures provide the only analogs for hands-on astronaut training or robotic exercises in preparation for fieldwork on other planetary surfaces. Impact structures not only represent the dominant surface features on, *inter alia*, the Moon, Mars, or asteroids but are also crucial for basic geoscientific surface analysis, subsurface geological studies, and analysis of sites of possible exobiological evidence or economic resources for future colonization of other planetary bodies. We assess 11 terrestrial impact structures of varied age, type, size, and erosion level, the majority of which have already served for astronaut or geoscientist/student training purposes, for their suitability as possible impact geological training sites. This evaluation is achieved through a range of (1) practical criteria (such as access time and site infrastructure) and (2) geological criteria (such as impact geology, target geology, aspects of impact cratering, outcrop conditions, and variety). For the practical criteria, Ries, Rochechouart, and Steinheim score the highest, with a small advantage for Ries. Sudbury and Meteor Crater score similarly, yet much lower than the leaders, with Vredefort in between. Talemzane and Araguainha are just below Meteor Crater. Clearwater West, Haughton, and Mistastin are by far the least suitable ones. Regarding geological criteria, the scores vary much less. The three Northern Canada structures and Steinheim are at the end of the record, yet only 23%–39% below Ries, which comes out as the leader and is closely followed by Araguainha (only 2% below Ries). Although the Northern Canada sites compare in size and type to the younger and less eroded Ries and the Araguainha (older and more eroded) structures, the diversity of impact features and lithologies and the outcrop situation are less favorable. Considering only the geological features and lithologies factors, Rochechouart gets the highest mark, followed by Araguainha, Sudbury, Vredefort, and Ries. In view of the targeted objective, the analog testing experiment places Ries and Rochechouart in the first and second positions, respectively. Steinheim and Vredefort score almost the same in the third and fourth positions, respectively. The three Northern Canada sites score the lowest. Based on their accessibility, relative proximity to each other, and remarkable complementarity in terms of crater type and size, and in terms of impact and target features and lithologies, the combination of the three leading structures (Ries–Rochechouart–Steinheim) may represent the most appropriate target for analog training purposes, from anywhere in the world.

KEYWORDS

planetary surface exploration, impact structure, terrestrial field analog, practical criteria, geological criteria

1 Introduction

After a period of mainly robotic exploration on the Moon and Mars, as well as remote-controlled asteroid probing, mankind is gearing up for renewed human exploration activities outside planet Earth. In the mid-2020s, the Artemis III mission of NASA is to restart human exploration on the Moon. Multi-faceted preparation activities are required for any such undertaking. The hostile planetary environments are just one challenge that preparation of astronaut crews will have to overcome. Knowledge of the natural environment to be encountered is another: fundamental knowledge of geoscience and different geological terrains is required. The surfaces of other planetary bodies that have been subject to long-term impact cratering modification can only be successfully investigated on the ground, if the concepts of impact geology and nature and genesis of the products of impact cratering, i.e., impactites and their generation, are understood. If a mission is targeting possible exploration for extra-terrestrial economic resources, concepts of ore formation must be well understood, together with the basic knowledge of hydrothermal processes. Impact geology and impactites will feature with high priority in the natural classrooms for the instruction of astronauts, and in the training of these amateur geologists, because of, *inter alia*, these main reasons:

1 Impact cratering is the fundamental accretionary process for solid bodies of the Solar System and beyond, having provided the building materials for planetary bodies as well as huge amounts of primordial kinetic energy to contribute to the effectiveness of planet differentiation.
2 Impact cratering has been the most important active geological process on the surfaces of the planetary objects most accessible to humankind.
3 The impact cratering process generates a variety of impactites (e.g., Stöffler and Grieve, 2007; Stöffler et al., 2018) and causes distribution of the products of impact in proximal (<5 crater radii) and distal (>5 crater radii) regions around source craters. Products of impact gardening (mass wasting of ejecta) include the regolith layer on the lunar surface, which has been considered a major economic resource for future lunar habitation and mining enterprises.
4 For the large planetary objects of the inner Solar System, impact cratering has been the main driving force of environmental change.
5 Impact cratering is a self-contained mechanism that could generate conditions conducive for the emergence of life even on seemingly inhospitable bodies (e.g., Cockell and Lee, 2002; Cockell et al., 2003).

In addition to impact geology, geological processes such as volcanism and tectonics, (faulting, folding, and brecciation) or hydrothermal activity are ubiquitous on the planetary bodies of the inner Solar System. For example, the surface of planet Venus is largely covered by volcanic rock and related products of impact cratering. Valles Marineris on Mars represents a gigantic fault system, the formation of which has been related to a combination of volcanic activity in the Tharsis region of Mars and associated tectonic stresses (e.g., Brustel et al., 2017). Hydrothermal activity must have taken place on Venus and Mars, in conjunction with their extensive volcanic activity. This would have been of major geological importance in relation to large-scale impact cratering events on these planets (e.g., Naumov, 2002; Abramov and Kring, 2004; Osinski et al., 2013; Simpson et al., 2020).

Astronauts and robots will walk and work on these planetary surfaces and must be capable of characterizing the different terrains and their geological components, in the context of the geological processes. This will require specific training in general and, more specifically, impact, geology, physics, chemistry, and even biology training. This can only be effective, if it is combined with enough field training, in order to learn how to recognize rock types, to follow and map contacts between different lithologies, and to identify geological structures such as faults, folding, veins, dikes, and sills, in order to allow basic geoscientific interpretation. In addition, trainees have to self-locate themselves in space, carry out sampling programs, collect appropriate field measurements, and more. Robotic equipment must be tested and equipped to carry out geological field programs independently. In this context, and for obvious practical and economic reasons, the terrestrial impact cratering record (i.e., currently approximately 210 confirmed structures; Gottwald et al., 2020; Kenkmann, 2021; Osinski, 2022) represents the only readily accessible resource for impact-related field training of humans and robots, and for testing of instruments.

The purpose of the present contribution is to assess a selection of terrestrial impact structures that might be used in future for such training purpose, and how they may contribute and provide potential "end-users" with a means to evaluate what training opportunities this selection has to offer. The impact structures chosen for this exercise have already been used in past decades for astronaut training purposes or are currently considered to serve this requirement. Several others are known for a wide variety of impact geological features and have already served extensively for geoscientist/student tuition.

How can such structures be assessed for their individual values? Where and why would they represent the best suited locations for satisfying specific training requirements? Of course, these requirements may be highly diverse, as they depend on the targeted planetary object, the specific mission objective(s) assigned to astronauts, robots, or instruments, and the time and budget that are available for field training. There is at least one requirement that is common to all those involved in the exploration of nearby planetary objects: the basic requirement to experience real rocks, their assemblages, and physical characteristics, all related to the mechanisms active in the formation and subsequent degradation of an impact structure.

We have developed a methodology for evaluating suitability of terrestrial impact structures for field training exercises using two categories of criteria—practical (or logistical) and geological criteria (GC). A large proportion of the terrestrial impact record is not appropriate for the proposed exercise because of the size (being too small), the setting (such as marine, buried under sediments, and deep erosion), or accessibility (e.g., remoteness or locations in conflict regions). Obviously, we are conscious of the fact that we are comparing a suite of impact structures of widely different characters: some of the oldest ones known on Earth (Sudbury and Vredefort) and rather young ones (Meteor Crater and Talemzane), which directly translates to (i) strongly degraded (most notable at Vredefort) or fresh in morphological appearance;

(ii) simple bowl-shaped structures (Meteor Crater and Talemzane) *versus* all other types of complex crater geometries; (iii) structures with crater fill preserved (e.g., Araguainha, Clearwater Lakes, and Haughton Dome) or essentially degraded to, close to, or beyond the crater floor (Vredefort). In addition, the selected candidate structures are formed in different target crusts (sedimentary, mixed sedimentary/crystalline, or crystalline targets), which affect not only the resulting crater morphology and scaling but also impactite formation.

For the purpose of this study, we have avoided to operate with scaling coefficients in order to present first-order observations and direct comparisons between attributes for these individual structures. Another aspect that should not be forgotten is the wide range of purposes that a developer of field campaign agendas may have to consider, for example, introduction to geology and geological techniques, specialized tuition about impact cratering processes and products, testing of equipment for planetary expeditions, and geophysical methodology. Thus, our parameters may only represent *one suite of evaluation criteria* that could be applied and that may have to be replaced or amended where appropriate. In any case, this present work is essentially focused on impact and target geology.

2 Field analogs

The terrestrial impact crater record currently counts some 210 officially confirmed impact structures (Schmieder and Kring, 2020; Gottwald et al., 2021; Kenkmann, 2022; Osinski, 2022). A small number of these sites have already been used for training astronauts and/or testing equipment. On the North American continent, Meteor Crater (also known as Barringer Crater, United States) has already been utilized since the 1960s (Kring, 2010). In Canada, Sudbury was visited by Apollo astronauts and has been a part of the program of the Canadian Space Agency for training astronauts, together with other Canadian sites that have received and/or are earmarked to receive geology field training expeditions for astronauts (Clearwater Lakes, Haughton Dome, and Mistastin). In Europe, the Ries Crater (Germany) had been used by NASA for geology training of astronauts already in 1970 (Kring, 2010; Phinney, 2015) and is currently used by ESA for the same purpose (Mangold et al., 2022; Sauro et al., 2022).

The present comparative evaluation of possible candidates for future training programs in impact geology is focused on these mentioned structures, but they are also compared against the Araguainha impact structure (Brazil) because it is the largest impact structure in South America, with a complex crater morphology and excellent exposures; Rochechouart (France) because of the recent significantly increased interest in this impact structure by the impact cratering community; the Steinheim impact structure (Germany) owing to its proximity to the Ries Crater; the Talemzane Crater (Algeria) because, just as Meteor Crater, it is a recent, simple bowl-shaped impact crater in a desert terrain, which is quite accessible from Europe and Africa; and finally, the Vredefort impact structure (South Africa), which is the largest known impact structure on Earth, has been well studied, and is the only terrestrial impact structure appearing in the UNESCO World Heritage list.

The following provides concise descriptions, given in alphabetical order, for this selection of analog structures. The salient facts and pertinent references about these candidate structures are summarized in Table 1.

However, a word must be added regarding the pertinent recognition criteria for impact structures. In addition to the presence of remnants of the meteoritic projectile at a crater site, there are only three reliable recognition criteria that allow to classify a suspected structure as a confirmed impact structure: 1) presence of shatter cones, 2) presence of diagnostic shock metamorphic features such as planar deformation features, or high-pressure polymorphs such as coesite or stishovite after quartz, or reidite after zircon, in the uppermost crust, and 3) evidence for a chemical/isotopic trace of a meteoritic (projectile) component in impact melt breccia. These criteria, or more generally what constitutes reliable evidence for impact and what does not, have been detailed, for example, by French and Koeberl (2010) and Koeberl (2014).

2.1 Araguainha

The 40-km-diameter Araguainha structure is South America's most prominent impact site (see Table 1; Figures 1A, B). It displays excellent exposures, especially since the MT-100 road crosscutting the structure was paved in 2021–2022. Th access is good, although the structure is rather remote from large cities. Since the 1970s, Araguainha has been continuously investigated (see Crósta et al., 2019). One intriguing aspect of Araguainha is the age for this impact, which is currently placed in the range from 252 to 259 Ma (Hauser et al., 2019). An age of 252 Ma would place this impact event of significant magnitude close to the age for the largest known mass extinction event known in the terrestrial biostratigraphic record: at the time of deposition of the Permian–Triassic Boundary. Whether this impact event played a significant role in this extinction event has been variably discussed in recent years (Tohver et al., 2013; Schmieder and Kring, 2020).

The Araguainha structure is located 750 km west of Brasilia at the NE limit of the intracratonic Paraná Basin, straddling the border between Goiás and Mato Grosso states. Its geology and further details such as stratigraphy have been presented most recently by Crósta et al. (2019), Hauser et al. (2019), and Leite et al. (2021), and a succinct summary has been given by Gottwald et al. (2021). The structure has some good exposures of pre-impact geology and impact-generated structures and lithologies. Except for the MT-100 road that straddles the entire structure from SW to NE, the area has limited road infrastructure, and tropical vegetation and strong surface weathering have limited continuous outcrop. Nevertheless, the structure provides a large suite of highly instructive exposures (examples are given in Figures 1A, B).

The macrostructure of the entire Araguainha impact structure is somewhat similar to the morphology of the Vredefort Dome, which is, however, only the central uplift of the much larger Vredefort impact structure (see below Section 2.11). In comparison, Araguainha is less eroded than Vredefort, in that some crater fill is still accessible. The central uplift of Araguainha comprises an inner core of crystalline basement—an Ordovician pluton of alkali granite, which is surrounded by a belt of Neoproterozoic phyllites and meta-arenites of the Cuiabá Group. Particularly in the northern sector, the outer core is surrounded/partially covered

TABLE 1 Pertinent data about the selected impact structures for assessing their suitability as field training sites for future planetary mission planning and preparation.

Impact site	Country, state	Latitude	Longitude	Size (Ø) [km]	Age [Ma]	Target type and lithologies	Crater type	Impact confirmed by	Impactite	Important reference	Training for
Araguainha	Brazil, GO-MT	16°47′S	52°59′W	40	252–259	Sedimentary/crystalline: arenite, quartzite, schist, and alkali granite	Complex	Shatter cones and shock metamorphism	Polymict lithic breccia, suevite, impact melt rock, and pseudotachylitic breccia	Dietz and French (1973); Hauser et al. (2019)	Geologists, students, and international excursions
Clearwater West	Canada, Quebec	W: 56°12′N	74°30′W	32	290–300	Crystalline: granitoid (dolerite and gabbro)	Complex	Shock metamorphism	Suevite and impact melt rock	Dence (1964); Grieve (2006); Osinski et al. (2015); Schmieder et al. (2015)	Astronauts and geologists
Clearwater East	Canada, Quebec	E: 56°03′N	74°05′W	24	460–470	Crystalline: granitoid (dolerite and gabbro)	Complex	Shock metamorphism, projectile contamination	Not exposed	Dence et al. (1965); Palme et al. (1979); Schmieder et al. (2015)	
Haughton Dome	Canada, Nunavut	75°23′N	89°39′W	23	39	Sedimentary/crystalline: limestone, dolomite, evaporite, granitoid sandstone, and gneiss	Complex	Shatter cones and shock metamorphism	Suevite and clast rich impact melt rock	Robertson and Mason (1974); Osinski et al. (2005); Osinski and Spray (2005)	Astronauts and geologists
Meteor Crater	United States, Arizona	35°01′39″N	111°01′20″W	1.2	0.049	Sedimentary: arenite and quartzite	Simple	Shock metamorphism, meteorite debris	Polymict lithic breccia and ejecta blanket	Barringer (1910); Kring (1997); Kenkmann et al. (2014); Poelchau et al. (2009)	Astronauts, planetary geologists, and international short courses
Mistastin Lake	Canada, Newfound land	55°53′N	63°18′40″W	28	36.6 ± 2	Crystalline: anorthosite and granodiorite	Complex	Shock metamorphism	Suevite and impact melt rock	Taylor and Dence (1969); Grieve (2006); Mader and Osinski (2018)	Astronauts and geologists
Ries	Germany, Southern	48°52′09″N	10°34′41″E	26	14.8	Sedimentary/crystalline: arenite, limestone, marl, amphibolite, gneiss, and granite	Complex	Shatter cones and shock metamorphism	Suevite, impact melt rock, and polymict lithic breccia	Shoemaker and Chao (1961); Artemieva et al. (2013); Stöffler et al. (2013)	Astronauts, planetary geologists, geologists, international short courses, and international excursions
Rochechouart	France, Southwest	45°49′27″N	00°46′54″E	23	205 ± 2	Crystalline: gneiss and granite (granodiorite, amphibolite, and serpentinite)	Complex	Shatter cones and shock metamorphism, projectile contamination	Suevite, impact melt rock, impactoclastite, and polymict lithic breccia	Kraut et al. (1969); Kraut and French (1971); Lambert (1977a); Lambert (1977b); Lambert (2010); Lambert (2022)	Planetary geologists, geologists, geophysicists, international short courses, international excursions, and students
Steinheim	Germany, Southern	48°41′12″N	10°04′02″E	3.5	14.8	Sedimentary: sandstone, shale, limestone, and marl	Complex	Shatter cones, shock metamorphism	Polymict lithic breccia, suevite	Dietz (1959), Reiff (1977), Buchner and Schmieder (2010)	
Sudbury	Canada, Ontario	46°36′N	81°11′W	200	1849.3 ± 0.3	Sedimentary/crystalline: para-arenite, shale, schist, and granitoid	Complex (multi-ring?)	Shatter cones and shock metamorphism	Suevite and impact melt rock	Dietz and Butler (1964); Dressler (1984); Grieve (2006); Lightfoot (2016)	Geologists (MSc courses), Apollo astronauts, and international short courses
Talemzane	Algeria, Sahara	33°18′50″N	04°01′34″E	1.8	<3	Sedimentary: limestone, (clayish–sandy–limestone)	Simple	Shock metamorphism	Monomict breccia and ejecta (impact melt rock)	Lambert. (1975), Chabou (2019)	International excursions
Vredefort	South Africa, Central	27°03′S	27°29′E	250–300	2023 ± 4	Sedimentary/crystalline: arenite and quartzite, dolomites, granitoid, and diorite, *inter alia*	Complex (multi-ring?)	Shatter cones and shock metamorphism, projectile contamination	Pseudotachylite, pseudotachylitic breccia, and impact melt rock	Hargraves (1961); Gibson and Reimold (2008); Reimold and Koeberl (2014); Reimold et al. (2021)	Geologists, geophysicists, planetary geologists, and international excursions

10.3389/fspas.2023.1186173

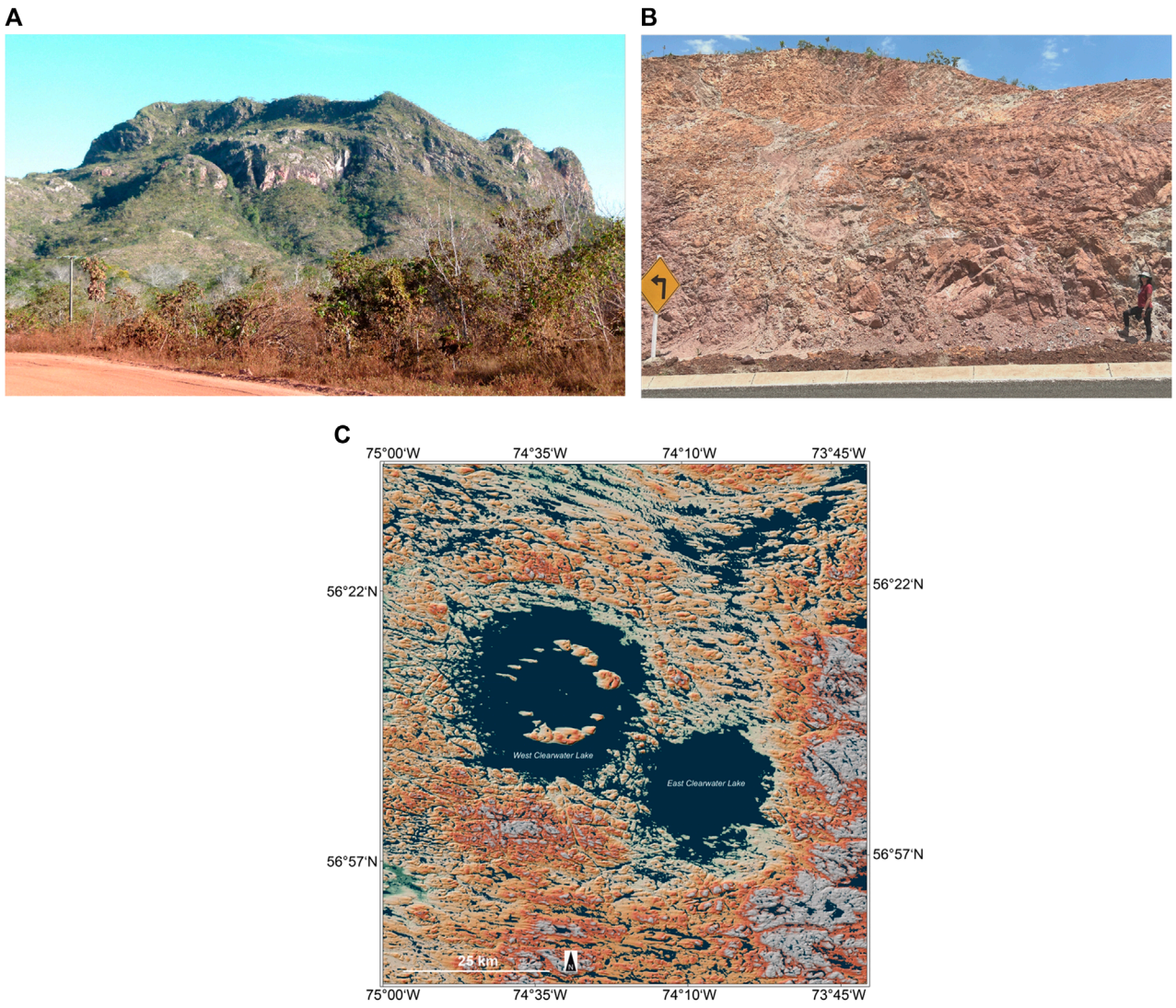

FIGURE 1
(A,B) Two scenes from the Araguainha impact structure in Central Brazil. **(A)** A hundreds-of-meters-sized megablock of the collar around the inner central uplift. This block represents Furnas Formation sandstone of the lower target stratigraphy. Field of view is approximately 600 m wide (in the background). **(B)** One of the extensive roadcuts generated in 2022 showing strong deformation of Cuiabá Group meta-arenite in the collar of the Araguainha central uplift. Note the person and road sign for scale. The greenish veins are still under investigation but seem to represent polymict impact breccia that may have been subjected to hydrothermal overprint. Photos: Wolf Uwe Reimold. **(C)** Clearwater East and West impact structures in Arctic Canada. Topographic map generated with the digital elevation model (DEM) of the TanDEM-X mission of the German Air and Space Institute (DLR). Image kindly provided by Manfred Gottwald/DLR.

by polymict lithic and suevitic breccia. The approximately 10-km-wide central core is surrounded by a broad syncline. In this zone, the upper target stratigraphy is exposed, which comprises a series of arenites and pelitic strata of the lowermost Rio Ivai Group and Furnas Formation, followed stratigraphically upward by the Ponta Grossa and Aquidauana Formations, and finally the Passa Dois Group. Whether the uppermost Corumbataí Formation of the basin sequence extended into the crater area prior to impact is debated. To the west and south, the environs of the structure are partially covered by ca. 134 Ma Serra Geral dolerite.

The clast provenance of the polymict impact breccias of the central uplift does not include much alkali granite material but seemingly a substantial load of blocks and megablocks of Cuiabá Group metasedimentary rocks, with some Furnas sandstone. Thus, there is currently a discussion about how deep the crater was excavated by the impact event. Shatter cones, an important recognition criterion for impact structures (e.g., Baratoux and Reimold, 2016), occur abundantly in Cuiabá phyllites and meta-arenites, as well as in many clasts of these lithologies in polymict impact breccia. Quartz in polymict breccia, and also in the alkali granite, carries planar deformation features. Shocked zircon has been discussed by Hauser et al. (2019) and shocked monazite by Erickson et al. (2017). Hauser et al. (2019) obtained electron back-scatter diffraction (EBSD) evidence for the presence of FRIGN zircon [former reidite in granular (zircon) neoblasts] from silicic melt rock clasts in polymict impact breccia. A meteoritic component

has so far not been identified from the impact-generated melt rock.

Melt rock occurs in two varieties at Araguainha. The alkali granite of the core contains numerous veins and dikes up to a width of 1 m, and up to tens-of-meters-wide pods of a dark gray-to-reddish melt rock (e.g., Machado et al., 2009). Quartz clasts are shocked, and an impact origin is beyond doubt. The chemical composition of this melt rock is essentially identical to that of the alkali granite. However, it is debated whether this phase represents injections or local formations of impact melt generated in the high shock pressure section of the transient crater, or whether it must be regarded as locally formed pseudotachylitic breccia akin to the veins and dikes of Vredefort. The latter is seemingly favored because of the absence of such material in suevitic impact breccia.

A second melt phase of highly siliceous composition, likely formed at the expense of quartzites and arenites of the lower Paraná Basin sequence, occurs as clasts up to meter size in the suevitic impact breccia. This melt phase has never been observed in alkali granite. Most of this material is strongly recrystallized, and formation of such siliceous melt must have involved very high temperatures. Consequently, shocked quartz is only rarely seen in such material, but shocked zircon has been described from it by Hauser et al. (2019). The Araguainha impact structure has long been suggested as a target for geopark development due to its significant regional geological record and its planetary geological context, at this dimension that is unique on the South American continent. Due to its remote location with regard to urban centers and limited infrastructure, such development has not been undertaken yet. However, in the past years, the MT-100 road, which straddles the entire Araguainha Dome from the SW to NE, has been upgraded and may form the basis for further investment into this eco- and geotouristic resource. This infrastructural upgrade has also resulted in accessibility to a series of outstanding roadcuts that provide study and mapping opportunities pertaining to all major impact-generated or impact-affected lithologies (polymict impact breccia impact melt rock, and target lithologies, with the exception of the alkali granite that is better exposed in the core of the structure).

2.2 Clearwater Lakes

The Clearwater Lakes impact site in northern Canada comprises two near-circular lakes, Clearwater East and West (Grieve, 2006; Schmieder et al., 2015; Biren et al., 2016; Rae et al., 2017), which are separated by a belt of islands (see Table 1; Figure 1C). The East Clearwater structure has a diameter of 24 km but no islands in the inner part. West Clearwater is larger, at a diameter of 32 km. The structure has a circular arrangement of islands at 6–10 km from the shore. Recent modelling has suggested an even larger crater diameter (35–40 km). For both the structures, significant exhumation by some 2 km has been suggested (Rae et al., 2017). Both lakes are characterized by negative Bouguer gravity anomalies that have been interpreted to indicate reduced density zones with impact-induced fracturing. Both structures also yield aeromagnetic lows over the crater regions. The structures have long been regarded as a rare example of double impact. However, age dating by Schmieder et al. (2015) has given the ages of ~286 Ma and ~460–470 Ma for the West and East structures, respectively.

Both structures are located approximately 110 km to the east of the SE lobe of the Hudson Bay. Full planning and preparation for an Arctic expedition are required prior to any visit to these sites. Access by seaplane is a must.

Clearwater East has numerous islands just inside of the lakeshore, which are considered part of the crater rim zone. Essentially underwater, this impact structure is not well exposed and most of the information on the impact rocks and shock features comes from two boreholes drilled at the center and 5 km off the center of the structure (Dence, 1964; Dence et al., 1965). Clearwater East is thus not considered for the purpose of this evaluation.

Clearwater West is a relatively well-preserved impact structure that was studied extensively in 1977 (Simonds et al., 1978; Phinney et al., 2015). More recently, the structure was revisited during a joint Canadian–US–UK expedition in August/September 2014 (Osinski et al., 2015).

The structure has a discontinuous remnant of the crater rim, with elevations of 50–100 m above the lake level. The circular array of islands has up to 100 m high elevations. A few islands in the innermost part of the lake have been related to a central peak. On these islands occur fractured parautochthonous basement and a variety of impact melt rocks and other impact breccias. The target was composed of various metamorphosed, 2.6–2.8-Ga-old granitoids of the Superior Province of the Canadian Shield. Metamorphosed and unmetamorphosed dolerites cut across this basement. Metagabbro occurs on the central islands. It is possible that Ordovician limestone formed a thin cover above the basement at impact time, as limestone blocks occur on the inner ring of islands and impact breccias contain some limestone inclusions. Impactites in evidence include shocked basement rocks with shatter cones, and impact melt breccia in the form of blocks up to 100 m in size. The structure has been drilled, and the crater fill includes, from bottom upward, fractured basement, impact breccias that include some suevite, and impact melt rock. The metagabbro contains diaplectic plagioclase glass (maskelynite), and the granitoids of the island ring contain quartz with planar deformation features. No meteoritic component has been detected in impact melt rock from Clearwater West.

2.3 Haughton

Haughton (or Haughton Dome) is located some 170 km from the Arctic town of Resolute Bay on Cornwallis Island in the High Arctic of Nunavut, Canada. Helicopter support and detailed arctic expedition preparations are thus required for field visits. Originally considered an evaporite dome, the structure was referred to as a possible impact structure in 1972 but confirmed only in 1975 through the discovery of shatter cones and coesite-bearing gneiss clasts in impact breccia (see Table 1; Figures 2A, B). Haughton is a 23-km-wide, 21–25 Ma, impact structure, which has been extensively explored for 40 years resulting in a large amount of data and literature (Grieve, 2006; Bischoff and Oskierski, 1988; Osinski and Spray, 2005; Osinski et al., 2005; for a recent review, see Gottwald et al., 2021). It is estimated that the structure has only been eroded by some 200 m. A strong fracture pattern encircles the structure, which makes it stand out prominently on satellite imagery.

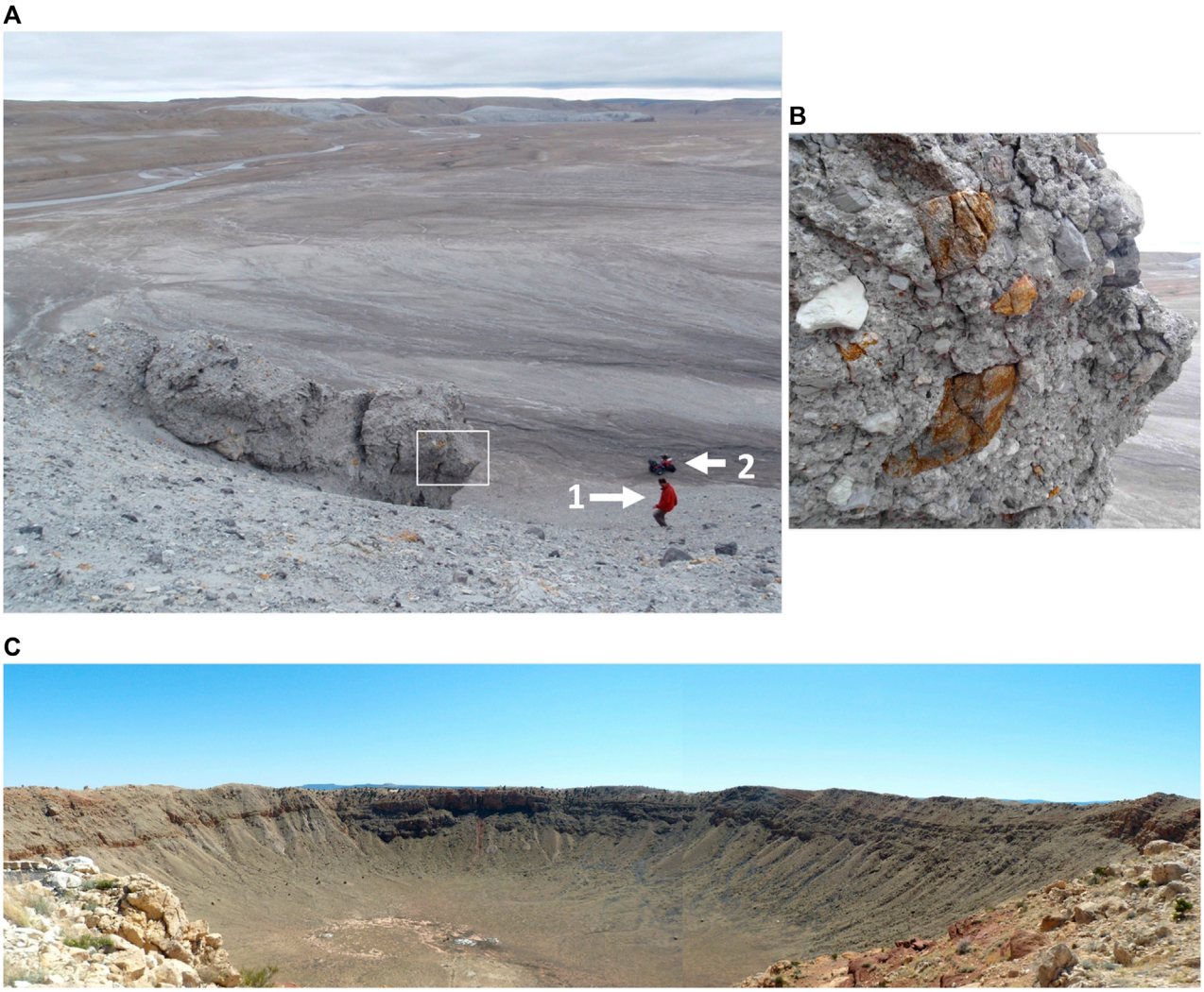

FIGURE 2
(A,B) Haughton impact structure, Nunavut, Canada. Images: Yoann Quesnel. **(A)** View showing a typical uniform landscape resulting from the alteration of the breccia. White square, field of view of **(B)**. 1, Geologist for scale, on his way downhill to his vehicle (quad marked 2). **(B)** Detailed view showing the polymict character of the main exposed impact breccia dominated by lithic clasts with metamorphic debris from the basement, up to 20 cm in size (rusty colored), mixed with sedimentary clasts (white). **(C)** Panoramic view of Meteor Crater, Arizona, United States, from the northern rim. Image: Philippe Lambert.

The target for this impact consists of a nearly flat-lying stack of 1,880 m of Lower Paleozoic sedimentary strata, above 2.5 Ga Archean metamorphic basement of the Canadian Shield. The basement includes predominantly tonalitic and granitic gneisses, with metasedimentary rocks, which were intruded at ca. 1.9 Ga by felsic plutons. All these Archean and Proterozoic basement rocks are cut by 600–800 Ma dolerite dikes. This basement is overlain by Middle Cambrian to Silurian sedimentary rocks, which include dominant limestone and dolomite, and subordinate evaporites, shale, and sandstone. Finally, post-impact lake deposits occur in the NW and SE sectors above impactites.

Regional gravity data indicate a central uplift, yet without topographic expression. The rocks within this inner, central uplift-related zone are Middle Ordovician to Upper Silurian strata that are strongly fractured, brecciated, and faulted. An inner ring with a diameter of 11 km marks the extent of the central uplift. This zone is surrounded by a depression with a diameter of 16 km, followed outward by a rim zone with inward-dipping normal faults and significant vertical throws on slump blocks. Impact lithologies include monomict impact breccias. Allochthonous ejecta and displaced material form polymict lithic breccia with clasts derived from basement rocks. Volumetrically dominant is an impact breccia filling the central crater, described as either a polymict impact breccia with clastic matrix (i.e., a lithic impact breccia) or as a clast rich, coherent, carbonatitic impact melt rock layer. The groundmass of this material consists of carbonate, silicate impact glass, and anhydrite. In the field and under the optical microscope, this breccia resembles polymict lithic breccia or melt-poor suevite and is clearly distinguished from impact melt rocks developed from crystalline target.

A meteoritic projectile could not be identified in the apparently melt-bearing rock. Shatter cones occur in great abundance at Haughton—in the area of the central uplift, within mega-blocks of ejecta, and in clasts of the allochthonous crater fill deposit. Occurrences of shock indicators such as planar deformation features in quartz, high-pressure polymorphs of silica, or diaplectic mineral glasses of quartz or feldspar are limited at Haughton, where the dominant target rock was carbonate facies. The structure shows abundant signs of hydrothermal mineralization, through deposits of secondary minerals in dissolution cavities, and along fractures in the impact breccias, in central uplift rocks, and along the faulted crater rim.

2.4 Meteor Crater

Meteor Crater, also known as Barringer Crater or Coon Butte, in Arizona, United States, is an extremely well-preserved impact crater of typical bowl-shaped morphology (see Table 1; Figure 2C. An excellent review was published by Kring (2017). Approximately 50,000 years (the preferred age) ago, an approximately 50 m sized asteroid impacted the flat plains of the southern Colorado Plateau. Numerous fragments of the "Canyon Diablo" iron meteorite have been collected in the environs of the crater of approximately 1.2 km diameter. The rim of the crater has been eroded by only 10–20 m. It rises some 30–60 m above the surrounding flat terrain. The flattish crater floor has accumulated some 30 m of erosion debris, which covers a thick lens of brecciated and melted rock. The rim section has been well studied in terms of structural deformation and contributed much to the general understanding of the structure of simple, bowl-shaped impact craters (e.g., Poelchau et al., 2009; Kenkmann et al., 2014).

Talus covers the lower parts of the inner crater rim wall but the upper 80–100 m of the steep wall is exposed and presents a stratigraphic sequence of Permian (Coconino Formation) to Triassic (Moenkopi Formation) sandstones. The rim sequence is partially uplifted and forms an "overturned flap" structure at the top, with inverted stratigraphy. There is an ejecta formation outside of the crater rim with blocky debris, which is responsible for the hummocky topography in the crater environs. The shape of Meteor Crater is not distinctly circular but rather squarish. This is the result of a prominent orthogonal joint system in the pre-impact target sequence, oriented parallel to the crater diagonals.

Much training for Apollo astronauts and geology and astrogeology groups has taken place at Meteor Crater. It provides a fresh example of the simple bowl-shaped impact crater morphology typical of impact craters <2 km (sedimentary targets) and <4 km (crystalline targets) in diameter on Earth. This crater morphology is ubiquitously found on the solid surfaces of planetary bodies in the Solar System, although on different bodies, the maximum diameters attained for simple, bowl-shaped structures vary (e.g., on the Moon, impact craters up to 20 km diameter fall into this morphological class).

In the early parts of the 20th century, Daniel Moreau Barringer had investigated the crater and its associated iron meteorites. He reached, and published in 1905, the firm conclusion that the crater was of impact origin, but this idea was rejected by the geoscience powers of his times (Barringer, 1910). Only in 1960, Chao et al. (1960) discovered the high-pressure polymorph coesite after silica in rock samples from Meteor Crater and thus vindicated Barringer's view. Detailed petrographic studies brought further confirmation in the form of shock metamorphic evidence, such as planar deformation features in quartz, and diaplectic and fused glasses after quartz.

Barringer had spent a lot of money in futile exploration, such as drilling of the crater floor, in a search for a large Ni-rich mass, with completely negative outcome. Today, it is well known that upon hypervelocity impact, the main volume of the impactor becomes vaporized, thus rendering Barringer's efforts useless. However, the Barringer family has since those days owned the land rights at Meteor Crater and has long run a very successful museum and visitors' center. Some of the proceeds from this highly profitable enterprise have been applied to support impact cratering research and especially, postgraduate student research and conference travel.

2.5 Mistastin

Mistastin (also Mistastin Lake) (Grieve, 2006; Marion and Sylvester, 2010; Mader and Osinski, 2018; Gottwald et al., 2021) is a complex impact structure with an apparent diameter of approximately 28 km (see Table 1; Figure 3A). This diameter is defined by some prominent hills considered remnants of the crater rim. The structure is rather eroded but still exhibits some indications of a terraced rim zone. The central part of the structure is mostly submerged by Lake Mistastin. The two large islands in the central part of the lake, Horseshoe and Bullseye, may represent the central uplift. The outer parts of the structure are mostly covered by up to 5 m of glacial deposits/soil and vegetation. The impact has been dated by Argon–Argon and U-Th/He geochronology to 36.6 ± 2 Ma.

The impact affected intrusive lithologies of the crystalline basement, which is dominated by granodiorite. Anorthosite, a rock prominent on the surface of the Moon, is well exposed on Horseshoe Island at the center of the structure and around the southeastern shore (Figure 3A). In contrast to the area outside, within the impact structure, the rocks are notably fractured. Despite vegetation and lake cover, the widespread exposure at Mistastin provides a good geological cross section through such a large, complex impact structure formed in a crystalline target.

A suite of impactites is accessible in the Mistastin structure, which includes shocked basement rocks, monomict impact breccia, polymict lithic impact breccia, suevite, and impact melt rock. Remnants of ejecta are mentioned in the literature. It is also possible to investigate profiles across the crater interior, between the lakeshore and apparent crater rim. In this zone occur steep changes in elevation, changes in fracture and fault patterns, varied prominence of exposure, and changes in the drainage system. Impact breccia occurrences are prominent along the shore of the lake, which includes a series of impact melt rock exposures. At a site in the southwestern sector of the structure, which is known as Discovery Hill, an 80 m high cliff of impact melt rock occurs. These impact melt rocks lie stratigraphically above allochthonous, lithic, or suevitic impact breccias, which themselves overlie parautochthonous, monomict brecciated basement. The crater floor rocks contain breccia dikes of impact glass, suevite, and pseudotachylitic breccia. The impact melt rocks are seemingly part

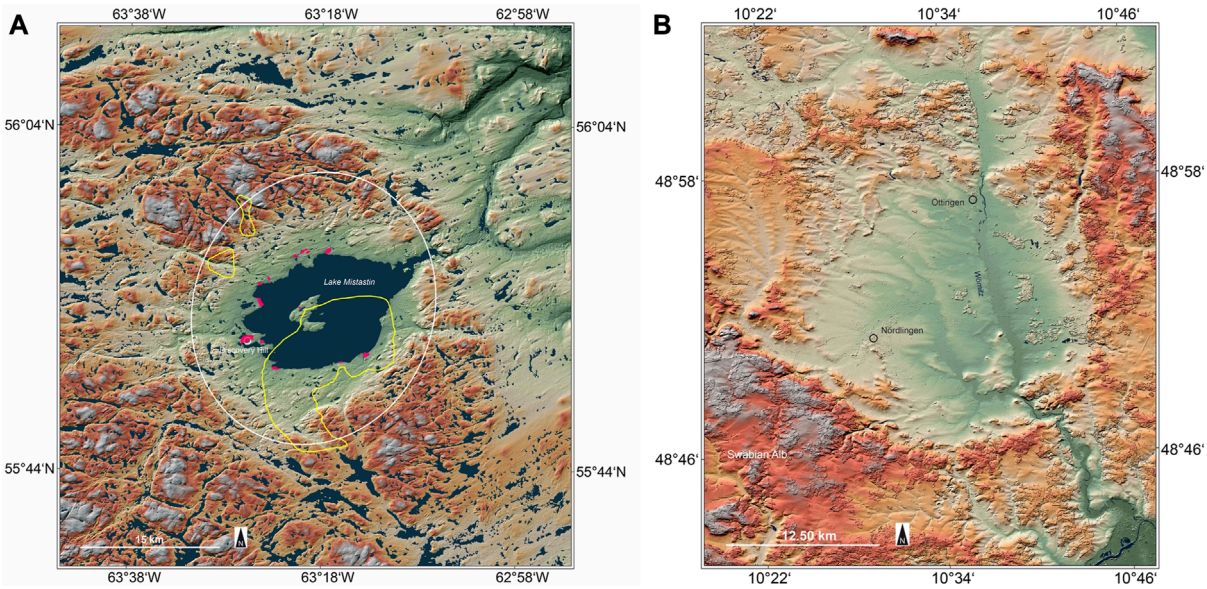

FIGURE 3
Topographic maps generated with the digital elevation model (DEM) of the TanDEM-X mission of the German Air and Space Institute (DLR). Images kindly provided by Manfred Gottwald/DLR. **(A)** Mistastin impact structure, Arctic Canada (red, impact melt rock occurrences; yellow lines emphasize occurrence of anorthosite; and the white circle indicates the apparent rim of the crater structure (after Mader and Osinski, 2018). **(B)** TanDEM-X based topographic map of the Ries Crater, southern Germany.

of a flat, sheet-like, and shallowly inward dipping body (e.g., Marion and Sylvester, 2010; Tolometti et al., 2022). Diagnostic evidence for impact genesis of this structure came in the form of shatter cones, shock metamorphic effects such as planar deformation features in quartz, and diaplectic quartz and feldspar glasses in basement rocks from the central islands. Extensive geochemical work on impact melt rocks has so far failed to provide evidence for the presence of a meteoritic component.

Mistastin is located in a very remote part of Labrador, approximately 120 km north of a place called Schefferville in Quebec. Access to the structure is limited to helicopter or seaplane support, and extensive expedition preparations will be required to visit and explore this impact structure which is used as an analog site for instruction by the Canadian Space Agency. In 2010, a robotic precursor mission documented the site, prior to a simulated human-sortie sample return mission with rover assistance that took place in the summer of 2011 with two astronauts (Marion and Sylvester, 2010).

2.6 Ries Crater

The Ries Crater (also known as Nördlinger Ries) in Southern Germany, in the region between the cities of München, Nürnberg, and Stuttgart, is one of the best preserved and best studied complex impact craters in Earth's impact record (see Table 1; Figures 3B and 4A, B).

Ries is known for its unique combination of proximal impact facies and a double-layer ejecta blanket, as well as an even more distal ejecta up to some 180 km into Switzerland. A tektite strewn field (with so-called Moldavites) extends to >400 km to the E/NE of the impact site. The structure has a number of excellent quarry exposures (Figures 4A, B). The 26-km-diameter structure comprises an almost circular inner depression, followed outward by an "inner ring" and a prominent "outer ring" (crater rim) that encircles some four-fifths of the entire structure. The crater structure is located against the Swabian–Frankonian Alb, a NE-SW trending major regional escarpment that existed already prior to impact.

The Ries impact has been dated on impact glass and moldavites to 14.8 Ma. The target sequence included a 650–750 m pile of Triassic–Jurassic to Neogene sedimentary strata above a basement of mainly pre-Variscan metamorphic rocks (ortho- and paragneisses and metabasites) and intrusives, mainly of granitic composition, of the Moldanubian Zone of the Variscan orogeny. In the Miocene, the southern part of the target area was covered by sands and shales of the Molasse Basin. Gottwald et al. (2021) described the pre-impact landscape as dominated by the Jurassic NE-SW trending escarpment of Malmian limestone. The inner crater basin has been extensively drilled, and the entire crater fill and some basement below have been intersected in the major research drilling "Nördlingen 1973". Below some 200–400 m of post-impact lake deposits, a 300 m succession of melt fragment-bearing impact breccia, the so-called "suevite" (Osinski et al., 2010; Artemieva et al., 2013; Stöffler et al., 2013), for which the Ries in the region of Schwaben (Suevia in Latin) is the type locality, follows. This is underlain by strongly fractured and brecciated crater floor above largely undeformed basement. The inner ring of the structure consists of uplifted basement rocks that are in part covered by lake sediments. The inner ring is surrounded by the 7–9-km-wide "megablock zone," with large blocks slumped off the crater rim that are partially covered by impact ejecta. The latter comprises a polymict lithic breccia with subordinate melt content, the so-called Bunte Breccia (variegated breccia), and megablocks

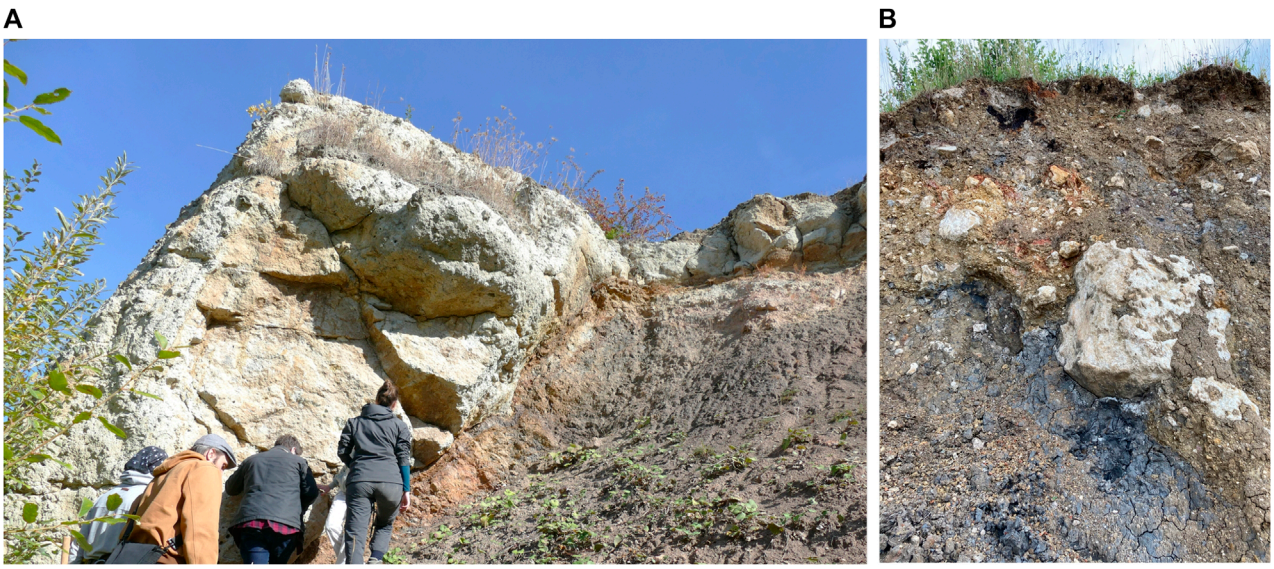

FIGURE 4
Two images from the Ries Crater kindly provided by Gisela Poesges. **(A)** Aumuehle Quarry. On the left, light gray suevite embedding a 2 m clast of limestone, lying above the brown Bunte Breccia (on the right). Field of view approximately 8 m. **(B)** Detail of the polymict lithic breccia termed "Bunte Breccia," with a variety of predominantly sedimentary rock clasts, from the Gundelsheim Quarry to the east of the Ries Crater. Field of view approximately 3 m wide.

of sedimentary and crystalline provenance. Steep concentric faults along the crater rim separate the inner parautochthonous units from the autochthonous rim strata.

Suevite, a mixture of clastic, unshocked to highly shocked debris with a sizable component of impact-generated melt fragments, occurs both as crater fill (crater suevite) and up to 30 km from the crater structure. Its clast population includes both crystalline and sedimentary target provenance but in contrast to the Bunte Breccia that occurs up to 45 km from the crater rim, the crystalline clast proportion of suevite is vastly higher. Studies of the Ries suevites and Bunte Breccia have contributed much to the understanding of how polymict impact breccias form in this highly dynamic cratering process. Suevite in the eastern and southern sectors of the crater carries a few patches of impact melt rock.

The Ries Crater has been geologically investigated since the 18th century. Mostly crypto-volcanic/-explosive ideas were entertained for a long time to explain the genesis of this anomalous structure. Finally, the outcome of the initial investigations into shock metamorphism, i.e., the irreversible changes to rocks and minerals incurred under the extreme dynamic pressures and high post-shock temperatures caused in upper crustal rocks only by impact cratering (e.g., Stöffler et al., 2018; Stöffler et al., 2019) could resolve the debate about the genesis of the Ries impact structure. The identification of the high-pressure polymorphs of silica, coesite and stishovite, in Ries samples by Shoemaker and Chao (1961) was soon followed by recognition of further shock metamorphic effects. Recently, some good specimens of shatter cones have also been found in the Ries.

In 1970, NASA conducted geological field training for astronauts in preparation of the Apollo 14 and 17 missions to the Moon, in the Ries Crater. In 1990, a well-appointed Ries Crater Museum was opened in the city of Nördlingen, which has since provided a support structure for impact cratering workers and student groups from around the world. In 2005, the Geopark Ries was dedicated by the German GeoUnion, and in April 2022, the Ries Crater Geopark was elected a Global Geopark by UNESCO. The ZERIN—Zentrum für Rieskrater-und Impaktforschung in Nördlingen—has been a further support facility for the international research community and many universities in Europe and beyond. Among other collections, this facility hosts a major part of the Ries drill core archive.

The Ries Crater is located only 45 km NE of a second impact structure, the Steinheim Basin. Until recently, it had been widely accepted that these two craters were formed simultaneously. On the basis of limited indications for possibly different chemical compositions of projectile matter, two hypotheses were established: cratering either by a single bolide possibly composed of two different lithologies separated upon approach, or impacts by a 1.5 km asteroid that would have formed the Ries and a 150-m-sized satellite that would have formed the Steinheim Basin. In 2022, it was proposed that maybe there was a time gap between the two impact events, as there could exist evidence for two, possibly impact-triggered, seismic perturbations in the rock record of southwestern Germany (Buchner et al., 2022; Schmieder et al., 2022).

2.7 Rochechouart

Rochechouart is an eroded complex impact structure located close to the NW margin of the French Massif Central, characterized by rolling hills and cattle farming, some 150 km NE of Bordeaux and 350 km SSW of Paris (see Table 1; Figure 5). A 12-km-wide, flat-lying breccia lens marks the bottom of the impact structure, occupying topographic highs in the landscape. The structure was

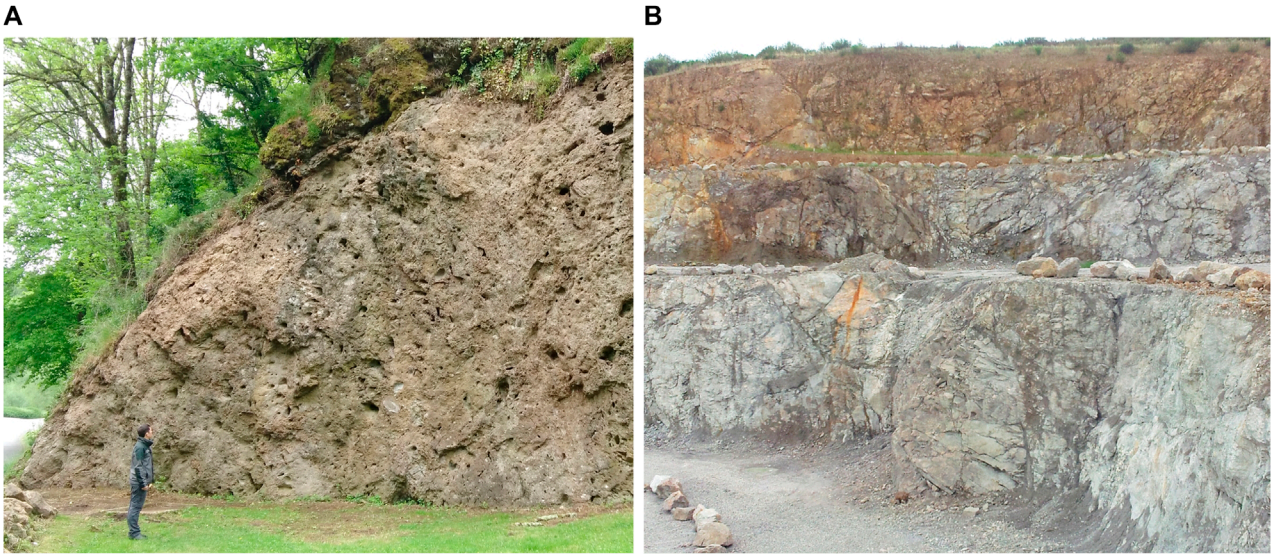

FIGURE 5
A section of the Rochechouart impact structure. **(A)** Outcrop below Rochechouart castle of a vesicular (vesicles could be related to outgassing of the hot impact breccia), melt-poor suevite (person for scale). **(B)** Champagnac stone quarry on the NE margin of the remnant of the crater fill deposit. Highly fractured, locally brecciated, dioritic basement strongly affected by hydrothermal fluids. Height of the quarry face approximately 90 m. Photos: Philippe Lambert.

formed in a crystalline target dominated by granites and felsic gneisses with local mafic intercalations. These lithologies were emplaced between ca. 550 and 300 Ma ago during the Hercynian (Variscan) orogeny (Faure et al., 2009; Lambert, 2010). The impact origin for the Rochechouart structure was first recognized by Kraut et al. (1969), based on the presence of shatter cones, shocked quartz, and diaplectic plagioclase glass, and later also supported by some traces of the meteoritic projectile in different impactites (Lambert, 1975; Janssens et al., 1977).

An intriguing aspect of the Rochechouart structure is the contrast between the advanced erosion that removed the entire crater topography and left only the remnants of the crater fill deposits, and the diversity of impactite facies still accessible. This is in part due to a unique feature of Rochechouart, where the level of erosion oscillates on both sides of the bottom of the crater. At other impact structures, the erosion levels are either at higher levels, and then the crater fill deposits are buried under later sediments accumulated in the crater, or the erosion level is comparatively lower, and then the crater deposits are entirely missing. Over a sub-circular zone of approximately 12 km width that marks the lowest region of the crater structure, Rochechouart exposes excellent cross sections through both the crater fill lithologies and the crystalline basement below. A large variety of target rocks dominated by felsic intrusive and metamorphic rocks are exposed. A complete series of impactites occurs at Rochechouart, which includes the so-called impactoclastite layer of fine rock and mineral debris that contains spherules thought to have been produced by condensation from the impact vapor cloud. Such spherules are rarely exposed in terrestrial impact structures but are known to form local to global deposits such as at the Cretaceous–Paleogene (K-Pg) boundary.

The variety of impact-related features in the target (such as shatter cones, shock veins, impact breccia dikes, pseudotachylitic breccias, and megablock formation) is often not complete at terrestrial impact sites. At Rochechouart it is. Throughout and even beyond the 12 km central zone, such features can be studied and provide information on all types of impact related mechanisms, which include localization of the deformation in the target related to shock compression, crater modification (central uplift formation and collapse), and late hydrothermal activity. Hydrothermal mineralization may, at some impact sites, be of economic (e.g., Naumov, 2002; Abramov and Kring, 2004; Reimold et al., 2005) and/or biological (e.g., Osinski et al., 2020) interest (habitability of planetary surfaces/emergence of life). Beyond macroscopic impact evidence, Rochechouart rocks record a full range of shock metamorphic effects at microscopic scales (e.g., Lambert, 2010; Plan et al., 2021).

The initial diameter of the Rochechouart impact structure is still debated. The "official" size is 23 km and corresponds to the zone where deformation found in the target rocks has been related to impact (Lambert, 1977a). More recent diameter estimates range, however, from 20 to 50 km, or even from 12 to 80 km (Lambert, 2022). Another intriguing aspect of Rochechouart is the age of this impact event, for which a range from 201 to 207 Ma has been given in the recent literature, close to the major mass extinction event in the terrestrial biostratigraphic record—at the Triassic–Jurassic Boundary (Tr-J) at 201 Ma.

Since the early 1990s, several local initiatives have drawn the attention of the public toward the heritage value of the Rochechouart impact structure. This resulted in the installation of a small museum at Rochechouart. In the early 2000s, the structure was awarded the European Geopark status by UNESCO, a label that was eventually lost because the minimum required local investments for maintaining the label were not met. However, in 2008, 12 localities representing major impactite units were placed under

the auspices of the French National Natural Reserve by the State, a curator was appointed, and the small museum in the town of Rochechouart became the House of the Reserve. More recently, the support of the international scientific community and local authorities has allowed the finding and equipping of a permanent facility in Rochechouart, which is dedicated to facilitating research and restitution on terrestrial impacts, in general, and Rochechouart, in particular. The Center for International Research and Restitution on Impacts and on Rochechouart (CIRIR) was thus created in 2016, with accommodation facilities, offices, laboratory equipment, and a sample library. Major accomplishments of the CIRIR are the facility development, establishment of management, and the realization of a first drilling campaign in the Rochechouart structure. This campaign delivered 540 m, on aggregate, of drill cores that have been made available to the scientific community (Lambert et al., 2019).

Furthermore, the first International Congress Festival (ICF-CIRIR 2022) and Asteroid Day-CIRIR-2023 were organized in June of 2022 and 2023, bringing together the scientific community and the public for several days at several localities across the impact site (Lambert, 2023). The Rochechouart structure is not only of great interest from an impact cratering perspective but also from an educational, social, and cultural perspective, owing to the philosophical, archeological, historical, and cultural values of both these events and the southwest region of France (Lambert, 2019; 2023).

2.8 Steinheim Basin

Steinheim Basin is a 3.8-km-diameter, complex impact structure on the Swabian Alb range of southern Germany, 45 km SW of the town of Nördlingen in the Ries crater. The Steinheim crater structure (Reiff, 1977; Reiff, 1979) is eroded but still somewhat preserved (see Table 1; Figures 6A, B). Steinheim represents one of the smallest complex impact craters known in the world. It was first proposed as an impact crater in the 1930s, which was later widely accepted after the relationship between shatter cones and impact structures had been established (first proposed by Dietz, 1959). Crater drilling also provided proof for impact in the form of planar deformation features in quartz from central uplift strata. There is an approximately 1-km-wide central uplift elevated by some 50 m above the surrounding ring basin. The crater rim is more subdued due to erosion.

The target stratigraphy at Steinheim consists of a sequence of sedimentary strata—limestone, shale, and sandstone—of Permian to Upper Jurassic age. The stratigraphic uplift in the center of the structure amounts to approximately 500 m. A crater fill breccia, known from drill core, lies on top of the crater floor. Locally, crater lake deposits form the uppermost stratigraphy in the crater. Blocks and boulders in the crater fill breccia carry abundant shatter cones. Fallback breccia of 20–70 m has been recognized by drilling. Both polymict lithic breccia and suevite have been identified.

Buchner et al. (2022) recently reported that there might be seismite evidence suggesting twofold "seismic shaking" in the stratigraphic interval of southwestern Germany that straddles the time of impact at Ries and Steinheim. They, thus, proposed that there may be a time gap between these two impact events and that the dual-impact hypotheses might have to be revised.

In the city of Steinheim am Albuch, the well-appointed so-called Meteor Museum informs about the geology of the crater, impact process, and post-impact resurgence of life into the impact crater, focused on the crater lake biome. The structure has several instructive geological sites with excellent explanatory boards. A day visit to the Steinheim Basin to learn more about the impact into a sedimentary target would be a welcome complement to geological study at the Ries Crater. Shatter cone findings are regularly made, especially on freshly plowed fields.

2.9 Sudbury

The Sudbury structure (Ontario, Canada), some 400 km north of Toronto, is one of the three largest impact structures known on Earth. Its original diameter, i.e., prior to tectonic deformation, was likely 200–250 km (see Table 1; Figure 6C). It is also one of the oldest impact structures known on Earth, with an age of 1,849 ± 0.3 Ma. Grieve et al. (2008) considered the Sudbury structure one of the only three likely multi-ring basin-type impact structures in the terrestrial impact record (also see Grieve, 2006; Lightfoot, 2016; Gottwald et al., 2021). Lightfoot (2016) also deals in detail with the economic geological aspects of this unique structure (also see Reimold et al., 2005).

The innermost part of the structure is known as the Sudbury Igneous Complex (SIC), which has a dimension of 27 × 60 km and a thickness of approximately 2.5 km. This complex represents a large body of differentiated impact melt (Therriault et al., 2002; Lightfoot, 2016). Around the SIC occur fractured/brecciated rocks of the crater floor. The crater floor is composed of Archean basement of the Superior and Southern provinces of the Canadian Shield, with good exposures in the environs to the north and east of the SIC. To the south, the SIC is surrounded by a belt of metasedimentary strata of the Proterozoic Huronian Supergroup. The Whitewater Group overlies the SIC and comprises impact breccias of the Onaping Formation, as well as post-impact sedimentary strata (mudstones and graywackes). In the lowermost parts of the SIC, the sublayer, as well as along the so-called Offset Dikes that represent impact melt intruded into the basement in the environs of the SIC occur large Cu-Ni ore bodies that in part contain important platinum group deposits. It has been estimated that the economic reserves include some 1.65 billion tons of Ni-rich ore, and that already a value of some 100 billion US$ has been taken out over some 100 years of mining at Sudbury.

Evidence for an impact origin of this formidable structure includes widespread occurrences of shatter cones all around and up to 17 km from the SIC (Figure 6D). The so-called Sudbury Breccia occurs in the form of numerous, and sometimes huge/massive, bodies of a melt rock that is thought to be equivalent to the pseudotachylitic breccias of the Vredefort structure (*sic*). Most Sudbury Breccia occurs within 5–15 km from the SIC, but the overall occurrence extends outward to 80 km from it. Sudbury Breccia is intriguing in its unique volume and by the variety of different breccia types that have been described (purely clastic breccia as well as melt-bearing types).

The breccias of the Onaping Formation overlying the rocks of the SIC have been variably interpreted as impact melt breccias and/or suevite. Supported by the mining industry, much geophysical

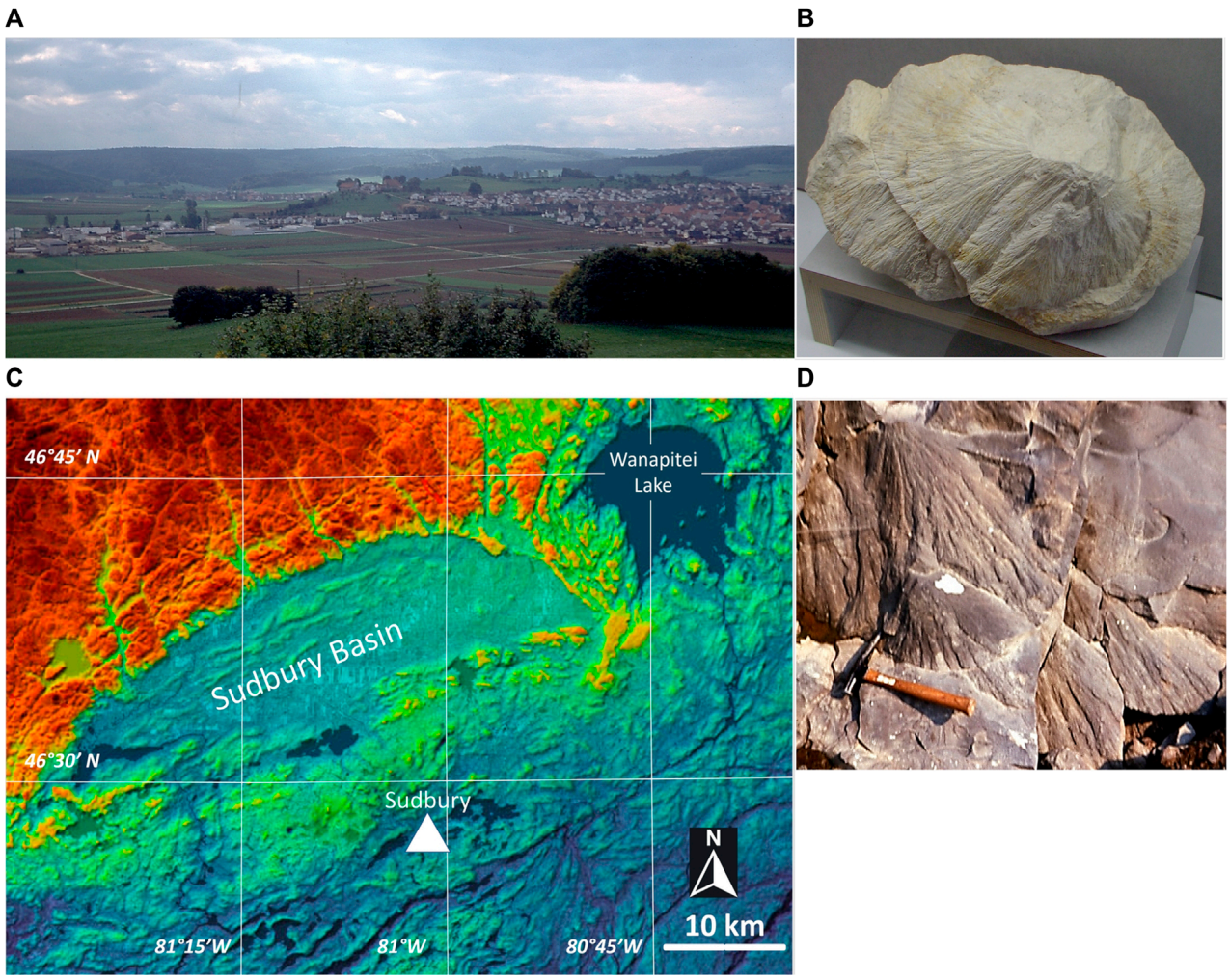

FIGURE 6
(A,B) Steinheim impact crater. **(A)** Panorama of the northern rim of the structure showing, at the center right, the central uplift against the town of Steinheim am Albuch. Field of view approximately 2 km wide. **(B)** Assemblage of highly detailed shatter cones in the Meteor Museum in Steinheim. This exhibit is approximately 50 cm wide. Photos by Philippe Lambert. **(C,D)** Sudbury impact structure. **(C)** Digital elevation model based on a NASA Earth Observatory image by Joshua Stevens, using topographic data from the NASA Shuttle Radar Topography Mission (SRTM) showing the Sudbury and the Wanapitei (at upper right) impact structures. **(D)** Shatter cones in quartzites of the early/mid-Proterozoic Mississagi Formation at a cutting at Ramsay Lake Road, a few kilometers from the Laurentian University. Photo: Philippe Lambert.

analysis across the Sudbury structure has been conducted, which includes extensive reflection seismic work. This resulted in a detailed three-dimensional assessment of the structure that showed that it is asymmetrical at depth. The reasons for this are that the structure was formed in the time of the Penokean orogeny and was also strongly affected by the 800 Ma later Grenvillian orogeny, both of which caused movement of strata in northwesterly direction, resulting in a shortening of the structure's diameter in this direction. Thermal metamorphism has strongly affected the rocks close to the SIC, and so evidence of shock metamorphism (e.g., planar deformation features in quartz) is only observed in a zone between 500 m and 8 km from the impact melt rock complex.

The Greater Sudbury Airport allows to fly into the structure, but it can also be reached on an excellent motorway from the city of Toronto. There are some very good exposures of shatter cones, Huronian metasediments, Sudbury Breccia, Sublayer and Footwall Breccia of the SIC, and Onaping impact breccias. Twenty-five kilometers to the NE of the city of Sudbury occurs a second impact structure, the approximately 10-km-diameter Wanapitei structure (Figure 6C). This structure is, however, essentially covered by Lake Wanapitei and does not boast impressive exposures. Suevite and impact melt rock blocks have been recovered from glacial deposits along the southerly shoreline.

2.10 Talemzane

Talemzane (Maâdna) (Belhai, 2006; Lamali et al., 2009) is a 1.75-km-diameter impact crater located on the northern Sahara platform, 390 km south of Algiers (see Table 1). The age of this impact has been estimated at 1 to 3 Ma (Lambert et al., 1975), possibly up to 5 Ma (late Miocene to early Pliocene) (Lamali et al., 2016). Talemzane was formed in flat-lying limestones with thin interlayers of clayish-sandy limestones of Eocene and Senonian age that were deposited 80 to

40 Ma ago. Extensively prospected by geophysics and drilled for oil exploration, the 3-km-thick sedimentary cover is known to be stable and free of salt tectonics (Busson, 1970; Fabre, 1974; Nedjari et al., 2002).

Although erosion has smoothed the rim, the structure still presents the morphological and structural characteristics of simple, bowl-shaped impact craters. The flat desert terrain of the Sahara platform, the complete absence of vegetation, and the smoothed morphology of the rim add to a Moon-like atmosphere (Figures 7A, B). Talemzane was first proposed to be an impact crater by Karpoff (1954) based on its circularity. Confirmation was then achieved on the basis of shock metamorphism by Lambert (1975). Further evidence for an impact origin, which included impact-generated carbonate melts, was reported by Sahoui et al. (2016).

The limestones in the crater wall are strongly fractured, uplifted, and locally overturned along the upper rim, and the crater wall is intersected by breccia dikes (Lambert, 1975). Impact ejecta are exposed on the outer flanks of the crater in the form of more or less cemented, fractured limestone blocks, up to several hundred meters from the rim. The crater is filled with alluvium that essentially masks all the crater fill. Monomict breccia is found locally on the rim and at the inner base of the rim wall. Melt-bearing breccia dikes are characterized by immiscibility textures between impact-generated carbonate-rich and silica-rich melt phases (Sahoui et al., 2016).

Just as Meteor Crater, Talemzane provides an excellent introduction to hypervelocity impact cratering mechanics related to relatively small projectiles, leading to bowl-shaped impact craters. With a smooth rim and a 40–70 m difference of elevation between the top and inner base of the crater wall, the relief at Talemzane is better suited for geological traverses by walking and perhaps robotic analysis than the relief at the younger, even less eroded Meteor Crater, where the upper crater wall is very steep. Also, Talemzane is relatively easily accessible. It is located 46 km ESE of the town of Hassi Delaa, which can be reached on a paved road from Algiers by regular car (6.5 h/500 km from Algiers International Airport). Yet, getting to Talemzane requires 4 × 4 transportation for dirt road travel and some off-road experience to avoid getting bogged down in the fesh-fesh (fine dust sand). It may take approximately 2 h for the 80 km from Hassi Delaa to the crater.

2.11 Vredefort

The Vredefort impact structure in north-central South Africa is the world's largest known and confirmed impact structure, with an original diameter estimated at 250–300 km (see Table 1; Figures 7C, D). The structure is centered at some 130 km SW of the Johannesburg International Airport. In addition to the detailed introduction to this structure by Gottwald et al. (2021), further information can be found in Gibson and Reimold (2008) and Reimold and Koeberl (2014). Largely due to the protracted debate about the origin of this unique structure, Vredefort has become one of the most widely studied and best characterized impact structures in the world. With a well constrained age of 2,023 ± 4 Ma (Kamo et al., 1996), it is also one of the oldest known structures in the terrestrial impact record. Extending from Johannesburg in the NE to the Welkom gold field in the SW, it largely corresponds to the erosional remnant of the Witwatersrand Basin (Frimmel, 2019), which was preserved with its economic resources due to impact-related downfaulting and cover by impact breccia.

The impact had occurred into an approximately 11-km-thick succession of supracrustal strata superposed onto the crystalline basement of the Kaapvaal Craton. The granitoids and associated lithologies of the crystalline core of the Vredefort Dome have been dated to >3.15 Ga. The lithologies of the innermost zone display granulite metamorphic grade, whereas the outer zone of the core is in amphibolite grade. The surrounding collar, in its inner segment, comprises strata of the Witwatersrand Supergroup (ca. 3.08–2.71 Ga), mostly meta-arenites and shales, as well as some amphibolites and banded iron formation of lower amphibolite to greenschist metamorphic grade. This sequence is followed outward by ca 2.71 Ga metavolcanics of the Ventersdorp Supergroup, and finally by dolomites and intercalated arenites of the 2.65–2.06 Ga Transvaal Supergroup.

The collar strata are extensively intruded by dioritic sills (the so-called *epidiorite*, metamorphosed to lower amphibolite facies) that have been related to the Ventersdorp volcanic–hypabyssal event. In addition, there are some occurrences of tholeiitic intrusions and several small alkali granitic and mafic–ultramafic complexes that have all been related to the Bushveld magmatic event at ca. 2.06 Ga.

That the Vredefort structure is of impact origin was first suggested in the 1930s and late 1940s, but this remained controversial until the 1990s. Whilst shatter cones had been reported in the early 1960s, it took until the mid-1990s to confirm the tell-tale indicators of shock metamorphism such as planar deformation features in quartz, shock deformation in zircon, and the presence of an admittedly very small meteoritic component in impact melt rock (e.g., Reimold and Koeberl, 2014; also see French, 1998; French and Koeberl, 2010). Since then, FRIGN zircon (former reidite in granular neoblasts, after zircon) has been added to this evidence (Kovaleva et al., 2021).

The Vredefort Dome is well known for its two types of impact-generated melt rock: pseudotachylitic breccia (PTB) and the Vredefort Granophyre. PTB was first described by Shand (2016) as "pseudotachylyte," a name that was later converted to "pseudotachylite" (= friction melt). Whilst there is a large community, also of impact workers, who favor friction melting for the genesis of this type of melt rock, also in impact structures, others have likened thin veins of this material with local occurrence of the high-pressure polymorphs coesite and stishovite at Vredefort to shock veins known from meteorites. Shock veins are considered to represent impact melt phases that were formed in the initial compression/decompression phase of the cratering process. However, the Vredefort Dome is famous for its massive occurrences of PTB, also well exhibited in a number of quarries (Figure 7D), and which are only superseded in volume by the Sudbury Breccia (*sic*). It has been discussed in recent decades whether these voluminous melt occurrences are not better investigated as likely decompression melts formed as a consequence of rapid uplift during the modification phase of impact cratering (for detailed discussion, see Reimold et al., 2016).

The second melt rock type of the Vredefort Dome is the Vredefort Granophyre, the true impact melt rock, which occurs in the form of nine dikes within the basement core and along the core/collar boundary. Recent discussions and reviews have been

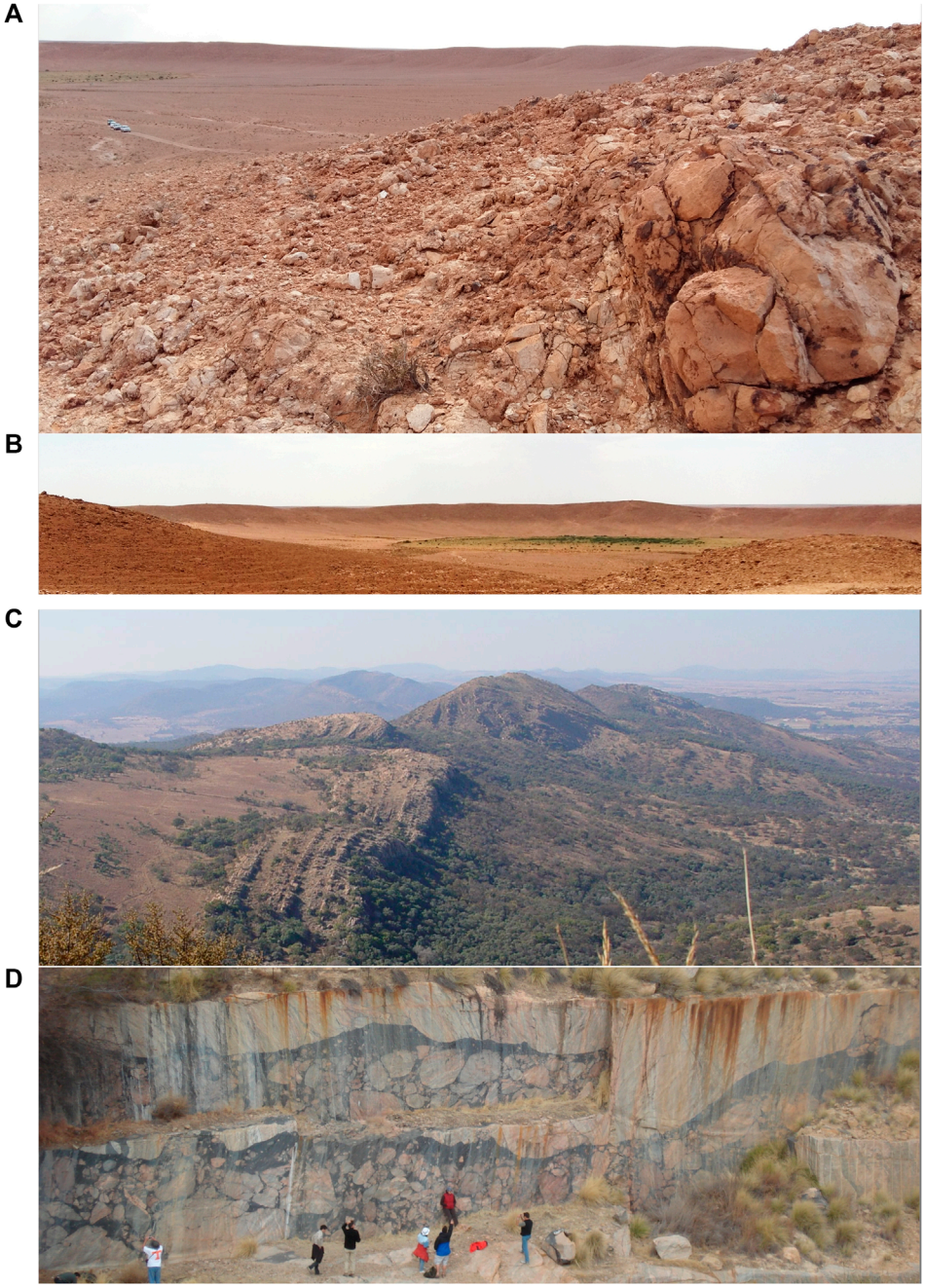

FIGURE 7
(A,B) Two scenes of the Talemzane crater. **(A)** Partial view of the crater from the northern rim, showing in the foreground, highly deformed and brecciated limestone with meter-sized blocks. Note cars for scale in the upper left. **(B)** Panoramic view of the crater from the northern rim. Width of field of view approximately 2 km. Photos: Philippe Lambert. **(C,D)** Two scenes that depict large-scale deformation features of the Vredefort Dome—the deeply eroded central uplift structure of the Vredefort impact structure. **(C)** View from Steenkampsberg in the western collar of the Dome toward the NW, across a scenic part of the Vredefort Mountain Land. The Hospital Hill quartzite has been slightly overturned and contains prominent deformation in the form of faulting and folding. **(D)** Impact cratering scientists (for scale) toiling in the Leeukop Quarry in the northern crystalline core of the Dome. This quarry allows a unique view onto a wide and massive development of pseudotachylitic breccia. The country rock here comprises various granite-gneiss types with local migmatite aspect.

published by Reimold et al. (2017, 2021, 2023). The granophyre dikes provide excellent exposures of impact melt rock. Two chemically different variants of impact melt rock, known as felsic and mafic granophyre, respectively, occur in two dikes in the northwestern sector of the dome Reimold et al. (2017, 2021, 2023). The reason for this duality is currently strongly debated, with either 1) consecutive intrusions of material from a differentiating impact melt sheet or 2) assimilation of a mafic country rock (epidiorite) by intruding felsic granophyre being favored (Reimold et al., 2021; 2023). These authors emphasize that chemical and isotopic data favor the latter

hypothesis. A granophyre dike on farm Daskop carries petroglyphs. The crystalline basement and partially massive pseudotachylitic breccias can be extensively examined in excellent quarry, and on some whaleback, exposures.

Due to the deep erosion of this large and very old impact structure, no remnants of proximal or even distal ejecta have been identified to date. However, it has been claimed (Huber et al., 2014; Huber et al., 2019; also see Allen et al., 2022) that Archean spherule layer occurrences in southern Greenland (Grænsesø) and in Karelia (Zaonega) could possibly represent distal ejecta from the Vredefort impact. The age constraints of these quite distant occurrences are, however, not sufficient for a positive ruling on this idea.

A portion of the Vredefort Dome was listed by UNESCO in July 2005 as a World Heritage Area, because of its outstanding geological, cultural, and historical record. A full inscription into the World Heritage listings has, however, not been achieved, as there are still management issues to be resolved. The structure is not only of great interest from an impact cratering perspective but also for general regional geological aspects, and its archeological and historical–cultural heritage (Reimold and Gibson, 2010).

3 Methodology for analog site evaluation

The proposed methodology relies on a series of (semi)quantitative criteria that fall into two main categories designated "practical criteria" and "geological criteria". The GC characterize the geological benefits of each analog site, whereas the practical criteria (PC) characterize their limitations and benefits on other grounds (see below). The latter are certainly an important aspect, as this category determines the feasibility of the training exercise and the time and efforts, indeed, ultimately, the cost, to be met for the establishment of an effective training program.

3.1 Practical criteria

The PC include the time required to get to the field analogs, related costs, and other practical limitations and benefits. A limited suite of departure sites from Europe, Canada, United States, Japan, and China is considered here for comparison of travel time and costs. For practical purpose, the starting locations are placed into capital cities. The mode of transportation considered is the most time/cost-efficient mean(s) required for reaching an impact site. Some sites can be reached from several international airports, and several simulations are proposed accordingly.

3.1.1 Time factor

Two factors are considered: TS, the time (hours) required to reach the site from the nearest major international airport (NIA), and TA, the time to reach the closest (time or distance) major international airport from the starting location. TA and TS rely on real time given by Google Maps for road transportation and by airline companies for air transportation, which include time and delays upon stopovers whenever applicable. The shorter the TS and TA are, the better suited is the analog site.

3.1.2 Cost factor

The cost factor (CF) considers two parameters: CS, the cost of transportation (material plus crew) to reach the site from the nearest major international airport, and CA, the cost of transportation (material plus crew) to the closest major international airport. The cost of transportation by road is based on car rental cost plus operating cost. The same base price applies to all destinations. The rental cost taken for a regular car is 50 €/day, transporting four persons, resulting in a cost of 12.5 €/day/person. The operating cost for a regular car is taken to be 12 € for 100 km, thus 3 €/person/100 km. The rental and operating costs of 4 × 4 transport is considered twice that for a regular car. Air fares are calculated on the basis of real prices proposed by commercial airlines when booking 6 months in advance, for the cheapest yet reasonably timed travel. Local transportation requiring the use of specific or private air carrier on all or part of the transportation from Ottawa–Montreal to Resolute Bay is taken at a conservative rate of 3,000 €/person with material, round trip. The cost of operating specific air transportation to the remotest Canadian sites is based on 1,000 €/h/person.

3.1.3 Other limiting factors

Five parameters count among other limiting factors (OLF) or those impairing the access to the field analogs, namely, political risk (PR), related to political instability and banditry; sanitary risk (SR) related to diseases, epidemics, distance to medical care; administrative constraints (AL) (authorization and escort requirements); environmental limitations (EL), such as topography, vegetation, and water; and weather conditions referred to as climatic risk (CL). The values for these parameters can be 0 for none, 1 for small, 2 for moderate, 3 for high, and 4 for very high risks. For CL, the values are 0 when the weather allows reaching and working on site all year around; 1 when it is not possible for 2 months or less; 2 when it is prevented for 2–5 months; 3 when it is not possible for 5–8 months in a year; or 4 when the site is inaccessible for approximately 9 months in a year or more due to climatic constraint. The smaller the factors are, the better suited a site is.

3.1.4 Benefit factor

This criterion characterizes the practical support that the end-user may find (or not) at a given site. It covers both the "living/accommodation" conditions and the "working conditions." The criterion for living conditions (LC) includes lodging, food, shopping, re-fueling, and sanitary support. The lowest mark 0 goes to a site where there is no living support available and to where everything (material for shelter, bedding, cooking, food, water, gasoline, medicine, heating and cooking fuel, etc.) must be transported. A mark of 1 is given for a site where poor living support is provided at some distance (1 h drive or more from the fieldwork area). A mark of 2 applies to sites where good living support is provided at some distance (1 h drive or more from the fieldwork area) and/or where living support exists on site but is poor/limited. The mark of 3 categorizes a site that offers good living conditions.

The criteria for working conditions (WCs) cover the availability on site of an impact dedicated museum and/or exhibits and didactic material (WC1), a sample library (WC2), drill core(s) (WC3), bore hole(s) available for training and testing (WC4), a dedicated facility with geological–geophysical tools, other equipment; laboratory directly available for users (WC5), and locally available expertise

(dedicated impact specialist(s) (WC6). All these factors directly contribute to reduce the requirements for the exercise and thereby the cost. The marks WC1 to WC5 can take are 0, none; 1, some; 2, good; or 3, excellent support. The values for WC6 are 1 if dedicated impact expertise exists on site and 0 if none is available. The larger the numbers are, the better suited a site is.

3.1.5 Marking rules

For the evaluation, all factors had to be homogenized and normalized to a common scale. For practical purposes, they are scaled to 4. For scoring the time and cost efficiency, we only consider access to the site from the nearest international airport (NIA). For all sites but Araguainha, Talemzane, and Vredefort, two or more NIA have been identified (see the Results and Discussion section). In order to get a single mark, we take the average time and cost to each site from the various possible nearest international airports. Another choice could have been to only consider the capital city of the countries hosting the sites as "nearest international airport". Yet, for Canada, Germany, and United States, there are several major international airports with direct flights from overseas.

There is a wide range of time and cost values, for which we have chosen a progressive scale. The highest mark 4 for the time factor (TF) is given for mean access time to the nearest international airport, 2 h or less. The mark of 3 is given when the mean access time is twice longer, thus between 2 and 4 h; mark 2 apply when it is between 4 and 8 h; mark 1 applies when it is between 8 and 16 h; and eventually, 0 applies when it is over 16 h.

Conversely, the highest mark 4 for the cost factor (CS) is given when the mean access cost per person for a round trip to the nearest international airport is 50 € or less (based on an occupancy of four persons for travel by car). Mark 3 is given when it is between 50 and 100 €; mark 2, when it is between 100 and 200 €; mark 1, when it is between 200 and 400 €; and eventually 0, when it is more than 400 €.

3.2 Geological criteria

The GC selected for evaluation of the suitability of any given impact structure for field exercises are quite diverse. Obviously, different field training programs, of which impact geology studies may only be one, may focus on different subjects such as 1) general geological tuition, 2) geophysical instruction, 3) field orientation and structural geological analysis, or 4) equipment testing. Some, and from case-to-case, varied criteria may not be of equal importance for these different purposes, so suitability of a given structure may be ranked overall by applying values according to the relative significance of the applicable criteria regarding each case.

For the purpose of the present exercise, we focus on impact geology field programs, keeping in mind that impact geology and impact-related mechanisms (translating into physical and chemical modifications of rocks), during and after cratering, and until the impact energy is fully released and the crater has cooled off, necessarily interfere with pre- and post-impact geology. Thus, a variety of geology fields (such as cartography, geomorphology, stratigraphy, petrography, metamorphism, structural geology, geophysics, and sedimentology) are not explicitly covered here but may find entry into impact geology field training programs. These aspects are to some degree, however, considered in the "Geological criteria" section in the context of the Geological Features and Lithology factors of the pre-impact target.

The GC applied here characterize an entire structure and are considered as averages of what the entire structure has to offer in terms of geology tuition. Criteria are distinguished under three categories: crater preservation (CP), outcrop situation (OS), and geological features and lithologies (GFL).

For CP, the mark 5 is for an impact crater where the initial topography and ejecta are intact (e.g., Meteor Crater), 4 is for a crater with minor degradation (smoothing of the rim, partial erosion of the ejecta blanket), 3 is for a strongly degraded crater that may still have some topographic expression (rim poorly preserved, ejecta essentially lost), 2 is for a deeply eroded crater (there is no more topographic expression, but the crater fill may be partially preserved and allochthonous impact breccia fill within the crater can be observed), 1 is for a crater deeply eroded below the crater floor (no crater fill deposit preserved), and 0 is for no exposure (e.g., structures buried under sedimentary deposits or under the sea).

The OC criteria are intended to characterize the average value of the outcrops on "practical grounds." This is independent of the geological interest that is evaluated separately and is covered by the GFL criteria. The OS considers two factors: 1) the quality of outcrop in terms of the amount of exposure and state of preservation. The related mark can take three values: 3, high; 2, moderate; and 1, low. 2) How much can be learned from outcrops in two full days of fieldwork. This criterion, thus, includes the number and variety of lithologies and features that the site has to offer, the accessibility of various outcrops, which may depend on vegetation, relief, water, road, trail, etc., and which also depends on distance to cover and what means of transportation may be required between stops—in essence, with relation to the size of a structure.

The GFL factor evaluates the tuition value of the major features and lithologies related to impact and target (see list below). The tuition value of a structure relies on the relative abundance and diversity of the features and lithologies—*as exposed in the field*. The quality of exposure is not relevant here (it is taken care of in the "Outcrop situation" section). Occurrence in drill cores or inference from geophysical data are not relevant either for the selection of these criteria. Yet, they are considered as benefits in the "Practical criteria" section.

For impact features, IFL (Impact Features and Lithology) marks are given for:

1. Ejecta blanket
2. Ejecta block
3. Overturned flap (rim)
4. Wall exposure and features (bulking, fracturing, and slumping)
5. Crater fill deposit
6. Polymict lithic breccia
7. Suevite (melt clast-bearing lithic breccia)
8. Impactoclastite (very fine-grained lithic breccia-bearing spherules and microcrystites)
9. Impact melt layer (large outcrop or zone where only impact melt rocks occur)
10. Impact melt rock and impact melt breccias
11. Crater floor exposure (e.g., the contact zone crater fill/basement is directly exposed)
12. Crater basement exposure

13. Central uplift (structural and or geological expression)
14. Megablocks
15. Monomict breccia
16. Shatter cones
17. Breccia dikes
18. Pseudotachylite (strictly used for friction melt) and pseudotachylitic breccia
19. Impact/post-impact economic mineralization
20. Impact/post-impact hydrothermalism

Target features and lithology criteria (TFL) rely on the relative abundance and diversity of features and lithological types of target rocks exposed in the crater area and/or up to 20 km outside of the structure, or the rim when it applies. These aspects include

Sedimentary rocks: Three major rock types are considered: 1, carbonate; 2, sandstone; and 3, others.

Intrusive rocks: Four major rock groups are distinguished: 1, felsic (e.g., granite); 2, intermediate (e.g., granodiorite and diorite); 3, mafic (e.g., gabbro); 4, ultramafic (e.g., dunite).

Metamorphic rocks: Four classes are considered: 1, felsic (e.g., quartzite and leptynite); 2, intermediate (e.g., schists or gneisses); 3, mafic (e.g., amphibolite and mafic granulite); 4, ultramafic (e.g., serpentinite).

Volcanic rocks: They are absent at our selected sites, but they may be added when necessary.

For all the entries, the possible marks are 0, absent; 1, low; 2, medium; 3, high. The GFL is the sum of impact features and lithology (IFL) criteria and target features and lithology (TFL) criteria.

4 Results and discussion

4.1 Practical criteria

4.1.1 Time

Supplementary Table S1 and related explanations in the Supplementary Material list the international airports located closest to our impact site candidates and give the distance in kilometers to the destination (and to intermediate stopovers when this applies). It also identifies the possible type of transportation, the corresponding time required, and the time required to reach the site which includes the time for stopovers where applicable. The type of transportation required on site is given as well. The most accessible impact site in terms of travel time from the nearest international airport is thus Steinheim from Stuttgart. Vredefort requires only marginally more time than the "Stuttgart–Steinheim standard". To reach Rochechouart is then 2 to 5 times longer, for Ries and Steinheim, 2–6 times; for Meteor Crater, 3–8 times; Sudbury, 5.5 times; Talemzane, 7 times; for Araguainha, it is 10 times longer; Clearwater Lakes, 12–19 times; Mistastin, 15–28 times; and for Haughton in the order of 36 times longer (Supplementary Table S1).

For a second, practical view, we consider the time required from a series of possible initial starting places, namely, the capital cities of China and Japan, major cities in Canada and the United States, and some capital cities of Europe. Supplementary Table S2 and Supplementary Figure S3 and explanations in the Supplementary Material give the shortest air travel time (TA) to the international airports closest to the selected impact sites from these various starting locations. As expected, starting from China and Japan results in the longest access time to all impact structures (Supplementary Figure S3). The total travel time is very similar for reaching both Vredefort and Talemzane from North America and from Beijing and Tokyo. To get to these structures is approximately 50% faster from Europe. The three Northern Canada impact structures are the candidates that require the longest overall time to reach, also from within Canada. Getting there from the United States, Europe, and Canada is not much different, reflecting the fact that it is not the access to the nearest international airport that dominates the result, but the time required to get to the impact site from the nearest international airport. Haughton is eventually the least accessible location in terms of approach time to the site.

4.1.2 Cost

Supplementary Table S4 and related explanations in the Supplementary Material allow to compare the round-trip cost per person for reaching the various impact sites from the nearest international airports either by ground transportation or by air (where it applies and/or is mandatory). As for the access time, we consider the cost to reach the selected analog sites from different countries (see Supplementary Table S5 and the details given in the Supplementary Material).

The three Northern Canadian structures are, by far, the least time and cost efficient of the selected impact structures. In addition, this finding is irrespective of whether the starting point would be from the nearest international airport within the same country, or whether it would be at other global hubs (Figure 8). There is a direct relationship between time and cost to reach the target structures. The time and cost histograms are homothetic (Figure 8). Yet, the range of variations is higher for cost than for time. The large difference between the three Northern Canadian sites and all the others, regarding time and cost efficiency, is reduced when departing from abroad (Figure 8).

4.1.3 Time and cost factors

The scores are given in Supplementary Table S6. As indicated before, the various sites rank in the same order for the two factors. It is Vredefort that gets the highest mark for both time and cost factors. The three European sites (Ries, Rochechouart, and Steinheim) also get the highest mark for cost factor (4). Yet, they score 3 for the TF. Araguainha, Meteor Crater, Sudbury, and Talemzane fall into the same category, with a 3 for cost and 2 for time. Eventually, the three Northern Canada sites score 0.

Supplementary Table S6 shows the relative time and costs from NIA, normalized to the shortest and cheapest. The access/cost ratio is a factor 2.5 or less for all sites but the Northern Canadian structures (Supplementary Table S6). This means that the cost is not such a discriminant. Even Araguainha and Talemzane are only twice as inefficient as Vredefort and Rochechouart, and not much different from Sudbury and Meteor Crater (Supplementary Table S6). The main difference is noted for the Northern Canadian structures, which are 30–120 times more expensive to reach than any other field analog considered in this study. The TF is more discriminating than cost between structures. The access/time ratio is approximately 2 for the three European sites, approximately 4 for Meteor Crater and Sudbury, near 5 for Talemzane, and near 7 for Araguainha (Supplementary Table S6). Eventually, the Northern Canadian sites

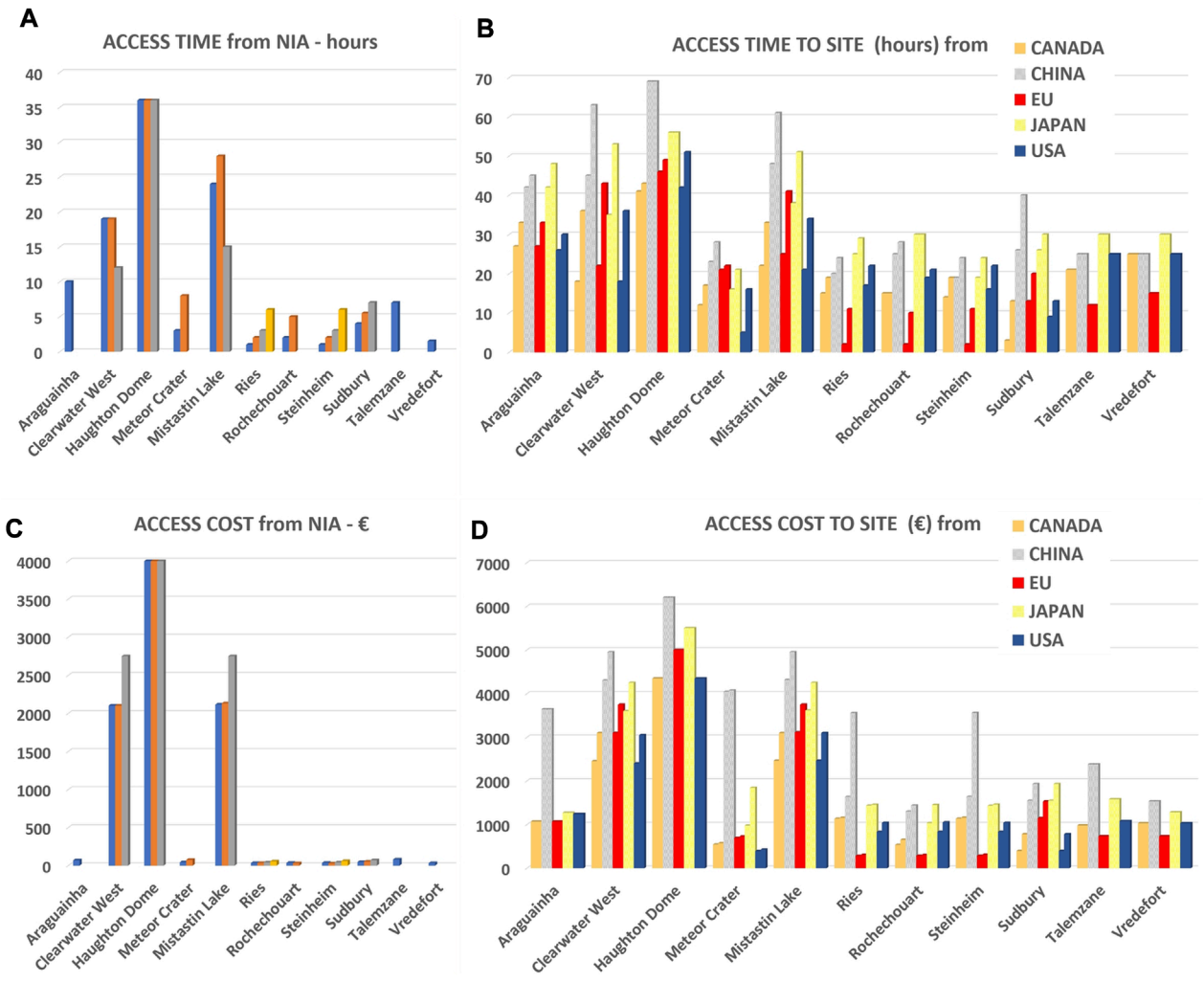

FIGURE 8
Comparing access time **(A,B)** and costs **(C,D)** to impact sites from the nearest international airports (NIA) **(A,C)** and from different international starting locations **(B,D)**.

are between 11 and 24 times less "access time efficient" than Vredefort.

4.1.4 Other limiting factors

The five parameters considered here receive marks between 0 and 4 (see the Methodology for analog site evaluation section). To enable the comparison and to be consistent with the scores for the other factors, the total for these individual marks is first inverted (so the highest numbers correspond to the most efficient sites), and the results are then scaled to 4 to give the consolidated mark for the OLF. The results are given in the Supplementary Material and summarized in Supplementary Table S7.

Overall, Ries and Steinheim receive the highest marks (4) for OLFs and score twice better or more than all other sites (see OLFr in SM7). Next comes Rochechouart scoring 2, then Vredefort with a score of 1.6, then Sudbury scoring 1.3, and Araguainha 1.1. Finally, Talemzane and the three Northern Canadian structures have the strongest limitations and score 5 and 7 times less than the two German sites (see OLFr in Supplementary Table S7).

4.1.5 Benefit factors

The detailed results for the seven benefit factors (BFs) are given in Supplementary Table S8. The aggregate BF values give Rochechouart the highest mark (4), followed by Ries with 3.1, and Steinheim with 1.9. With a mark of 1.2, Sudbury scores 3.4 times less than Rochechouart, Meteor Crater and Vredefort 5.7 times less, and Araguainha 8.5 times less than Rochechouart (see BFr in Supplementary Table S8). The Northern Canadian structures score 0.

4.1.6 Aggregate result for all practical criteria

The overall PC mark is obtained by combining, with an equal weight, the results for the four practical factors (TS, CS, OLF, and BF). The total obtained for each site is then normalized to the highest scores and scaled to 4. The resulting score for each factor is given in the table on the left in Figure 9A, and the distribution is graphically represented in Figure 9B, as proportions of the highest score.

One notes a high-scoring group with the three sites in Europe. Ries receives the highest score, closely followed by Rochechouart

A

	TS	CS	OLF	BF	PC
Araguainha	1	3	1.14	0.5	**1.6**
Clearwater West	0	0	0.57	0	**0.16**
Haughton Dome	0	0	0.57	0	**0.16**
Meteor Crater	2	3	1	0.7	**1.91**
Mistastin Lake	0	0	0.57	0	**0.16**
Ries	3	4	4	3.1	**4**
Rochechouart	3	4	2	4.0	**3.7**
Steinheim	3	4	4	1.9	**3.66**
Sudbury	2	3	1.33	1.2	**2.14**
Talemzane	2	3	0.8	0	**1.65**
Vredefort	4	4	1.6	0.7	**2.93**

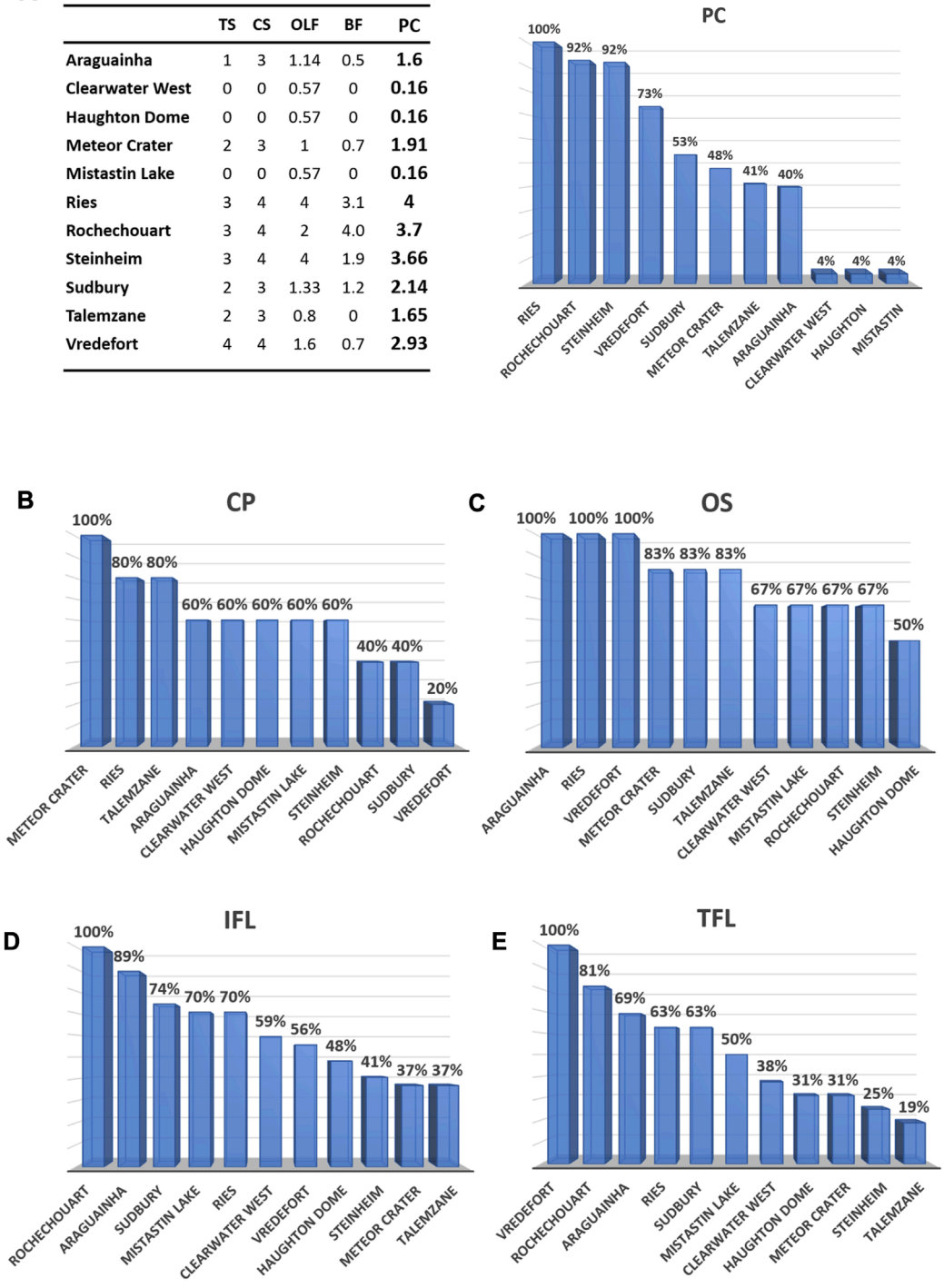

FIGURE 9
(A) Practical criteria. Marks for the individual factors taken from Supplementary Tables S1–3, and Supplementary Tables S6–8. TS, time factor; CS, cost factor; OLF, other limiting factors; BF, benefit factors. To the right: aggregate scores, i.e., the means of the four individual factors, used with the same weight, all scaled to the highest mark of 4. **(B–E)** Geological criteria factors from values given in Table 2, ranked by score, in proportion of the best score. **(B)** CP, crater preservation factor; **(C)** OS, outcrop situation factor; **(D)** IFL, impact features and lithologies factor; **(E)** TFL, target features and lithologies factor.

and Steinheim scoring 8% below Ries (Figure 9B). A relatively low mark (2) obtained for OLF penalize Rochechouart, despite it holding the highest mark for the benefit criteria. For Steinheim, it is a relatively low mark for the benefit criteria (1.9), when compared to Ries and Rochechouart, that accounts for the difference (Figure 9A).

Vredefort scores some 20% below Rochechouart and Steinheim and 28% below Ries (Figure 9A). Getting the highest mark for two of the four factors makes the global mark for the PC: Vredefort stands 20% above Sudbury and Meteor Crater, scoring 53% and 48% (see Figure 9A, right). If the threshold of mark 4 for travel time was raised to 5.5 h, and that for travel cost to 100 €, then Meteor Crater and Sudbury would get a 4 for the time and cost factors. If this does not change the scoring and ranking for Ries, Rochechouart, Steinheim, and Vredefort, it does for Sudbury and Meteor Crater. Their PC marks then fall just a little above or below the value of Vredefort. This illustrates the importance of the criteria settings. To reach Sudbury or Meteor Crater from the nearest international airport is approximately three times longer than getting to Vredefort from Johannesburg, and a little less than twice more expensive. Thus, while we stick with our results, the difference is a matter of a few hours and a few tens of Euros.

Figure 9A shows that Talemzane and Araguainha are both 60% below Ries and only 8% and 12% below Sudbury and Meteor Crater, respectively, both of which have already served as training sites for astronauts. A big gap separates Talemzane and Araguainha from the three Northern Canadian sites that are ranked 96% below Ries and some 35% below Talemzane and Araguainha.

4.2 Geological criteria

The GC characterize what an entire impact structure has to offer in terms of geology for field tuition. The criteria strictly rely on what is exposed in the field. There are three categories: CP, OS, and GFL, and in Table 2 the results for the various factors in each category are compared with the structures considered here.

4.2.1 Crater preservation

Due to the young age of Meteor Crater, crater morphology and ejecta blanket are rather well preserved at this crater, which thus deserves the highest mark (5) (compare Table 2). Talemzane and Ries are more degraded: rims and walls are smoothed, and the ejecta blankets are partially, although in the case of the Ries substantially, preserved. Their CP mark is 4. Araguainha, Clearwater West, Haughton, Mistastin, and Steinheim are more eroded. The rims are still in evidence, yet they are not well preserved, and ejecta are essentially lost. Their CP mark is 3. For Rochechouart and Sudbury, the crater topography has been lost, yet the crater fill is partially preserved and exposed in the field. They score 2. At Vredefort, erosion has essentially removed the entire crater structure and cut deep into the crater basement. However, the geological structure of a deep section through the central uplift and some impact-generated rock types are well exposed (see IFL-10 and IFL-18) and provides a unique cross section through the root zone of a very large central uplift structure. The mark for CP is 1.

The CP values in Table 2 are ranked in diminishing order as shown in Figure 9B, in proportion of the best scores. Clearly, the age–size relationship is most important. The best score is obtained by the youngest and smallest crater of the series (Meteor Crater), and the lowest score by the oldest and largest one (Vredefort). In between, the second-best scores are shared by Talemzane and Ries, the second youngest sites of the series. Talemzane is younger than Ries, yet Ries is larger, and their state of preservation is somewhat similar. The same applies to the four structures with intermediate scores at 60%: Clearwater West, Haughton, and Mistastin fall into the same size and age range, and compare, in terms of preservation, to the much smaller Steinheim structure. Araguainha and Rochechouart both compare in age and size, and compare in size with the three Northern Canadian structures; yet, they are older than Haughton and Mistastin. Rochechouart scores lower, yet Araguainha scores higher than the three North Canadian structures. This probably reflects the lack of sensitivity of the criteria, established on a scale from 0 to 5.

4.2.2 Outcrop situation

The outcrop situation is independent of the geological interest and relies on two factors: the quality of exposures and the variety of features exposed. This is also expressed by how much can be carried out in the field in 2 days. Regarding the first factor, the size and state of preservation of the outcrops, the situation at Rochechouart is poor. Outcrops are abundant and varied, yet most are small and relatively weathered, which gives Rochechouart the lowest mark (1) (Table 2). Conversely, the quality of exposure is excellent at all other sites, with the exception of Steinheim that is extensively covered by agricultural terrain and, thus, obtains an intermediate mark (2).

For the second factor, the variety of study aspects, Rochechouart receives a high mark of 3. The structure is distinguished by its wide range of target and impact lithologies, and associated features, exposed over a relatively small zone of some 10 km extent. There is generally easy and rapid access to outcrops of interest (close to roads or trails accessible by regular car and never more than a couple of hundred meters from the car). Despite excellent exposures, the three Northern Canadian impact structures are those where the least can be carried out in a field day because of the lack of access and the relatively large distances to cover. They deserve a mark of 1. Desert land at Meteor Crater and Talemzane provides excellent outcrop conditions. Yet, owing to their small sizes and young ages, the amount of tuition on offer is limited. They also obtain a mark of 1. At Steinheim outcrops are scarce, which delimits tuition possibilities (mark 1). At Vredefort and Sudbury, the outcrop conditions are good. Yet, these structures suffer from a deep level of erosion, and the large sizes of these structures limit, to some degree, how much can be carried out in 2 days. These large structures, thus, also get a mark of 1. Ries and Araguainha, which are comparatively smaller and less eroded, display a wide variety of features and lithology for a mark of 2.

The overall OS results are given by the sum of the two contributing factors for each site (see Table 2). As for CP, the OS results are plotted in diminishing order as shown in Figure 9C. The scatter of values is less than for the other geology factors, and there is no obvious trend in the scores. The leading scores are obtained by the very old and large Vredefort structure, the young and medium-sized Ries, and the relatively old (252–259 Ma) and medium-sized Araguainha structure. The score for the very old and very large Sudbury structure matches those for the two smallest and youngest impact craters and falls into the middle of the range. For these two youngest structures, the top quality of outcrops due to the desert environment is counterbalanced by their small size with limited variety of geological aspects. Crater size limits the amount of field tuition that can be carried out in 2 days. Had the limit been set to

TABLE 2 Marks for the Geological Criteria.

Geological criteria	Araguainha	Clearwater West	Haughton Dome	Meteor Crater	Mistastin Lake	Ries	Rochechouart	Steinheim	Sudbury	Talemzane	Vredefort
CP: crater preservation	3	3	3	5	3	4	2	3	2	4	1
5 = Perfect (topography and ejecta are intact), 4 = minor degradation (smoothing of the rim, partial erosion of the ejecta blanket), 3 = strongly degraded but still some expression (rim poorly preserved, ejecta essentially lost), 2 = deeply eroded, no topographic expression but crater fill partially preserved, 1 = deeply eroded below the crater floor (no crater fill deposit preserved), 0 = no exposure (buried)											
OS: outcrop situation											
3 = high; 2 = moderate; 1 = small											
Outcrop quality	3	3	2	3	3	3	1	2	3	3	3
How much can be carried out in 2 days*	2	1	1	1	1	2	3	1	1	1	1
OS: total	5	4	3	4	4	5	4	3	4	4	4
**referring to the number–variety of lithology/feature, the size of the structure, the accessibility of the outcrops (see text, Section 4.2)*											
GFL: geological features and lithologies											
IFL: impact features and lithologies											
0 = absent, 1 = small, 2 = medium, 3 = high											
IFL-1: Ejecta blanket	0	0	0	2	0	2	0	0	0	1	0
IFL-2: Ejecta block	0	0	0	2	0	2	0	1	0	1	0
IFL-3: Overturned flap (rim)	0	0	0	2	0	0	0	0	0	1	0
IFL-4: Wall exposure and features (bulking, fracturing, and slumping)	0	0	0	3	0	0	0	0	0	1	0
IFL-5: Crater fill deposit	2	2	3	0	2	2	2	0	1	1	0
IFL-6: Polymict lithic breccia	2	1	1	1	1	3	3	0	0	1	0
IFL-7: Suevite-melt-bearing polymict lithic breccia	2	1	3	0	1	3	2	0	1	0	0
IFL-8: Impactoclastite	0	0	0	0	0	0	1	0	0	0	0
IFL-9: Impact melt layer—columnar jointing	0	2	0	0	2	0	1	0	3	0	0

(Continued on the following page)

10.3389/fspas.2023.1186173

TABLE 2 (*Continued*) **Marks for the Geological Criteria.**

Geological criteria	Araguainha	Clearwater West	Haughton Dome	Meteor Crater	Mistastin Lake	Ries	Rochechouart	Steinheim	Sudbury	Talemzane	Vredefort
IFL-10: Impact melt rock	2	2	0	0	3	1	2	0	3	1	2
IFL-11: Crater floor exposure—contact crater fill/basement	2	1	0	0	1	0	3	1	1	0	0
IFL-12: Crater basement exposure	1	1	0	0	1	0	3	1	1	0	3
IFL-13: Central uplift—structural and or geological expression	3	2	1	0	2	0	1	2	0	0	3
IFL-14: Megablocks	2	1	1	0	2	3	1	1	0	0	0
IFL-15: Monomict breccia	1	1	1	0	1	1	2	1	0	1	0
IFL-16: Shatter cones	3	1	2	0	1	1	2	3	3	0	3
17: Breccia dykes and breccia veins	1	1	0	0	1	0	2	0	2	2	0
IFL-18: Pseudotachylite and pseudotachylitic breccia	2	0	0	0	1	0	1	0	3	0	3
IFL-19: Impact/post-impact economic mineralization (1 = yes, 0 = no)	0	0	0	0	0	0	0	0	1	0	1
IFL-20: Impact/post-impact hydrothermalism (1 = yes, 0 = no)	1	0	1	0	0	1	1	1	1	0	0
IFL: total	24	16	13	10	19	19	27	11	20	10	15
TFL: target features and lithologies											
(inside and outside the structure (up to 20 km away))											
0 = absent, 1 = small, 2 = medium, 3 = high											
Sedimentary											
TFL-1: Carbonates	1	1	3	3	0	3	1	2	0	3	3
TFL-2: Sandstones	3	0	1	2	0	3	1	1	1	0	0
TFL-3: Other sedimentary rocks	1	0	1	0	1	1	0	1	1	0	0

(Continued on the following page)

10.3389/fspas.2023.1186173

TABLE 2 (*Continued*) (*Continued*) **Marks for the Geological Criteria.**

Geological criteria	Araguainha	Clearwater West	Haughton Dome	Meteor Crater	Mistastin Lake	Ries	Rochechouart	Steinheim	Sudbury	Talemzane	Vredefort
Intrusive											
TFL-4: Felsic	3	0	0	0	0	0	3	0	0	0	3
TFL-5: Intermediate	0	0	0	0	2	0	1	0	0	0	0
TFL-6: Mafic	0	1	0	0	0	0	1	0	0	0	3
TFL-7: Ultramafic	0	0	0	0	0	0	0	0	0	0	0
Metamorphic											
TFL-8: Felsic	1	3	0	0	3	1	3	0	3	0	3
TFL-9: Intermediate	2	0	0	0	2	1	1	0	3	0	3
TFL-10: Mafic	0	1	0	0	0	1	1	0	1	0	1
TFL-11: Ultramafic	0	0	0	0	0	0	1	0	1	0	0
Volcanic	0	0	0	0	0	0	0	0	0	0	0
TFL: Total	11	6	5	5	8	10	13	4	10	3	16
GFL: Total	35	22	18	15	27	29	40	15	30	13	31

10.3389/fspas.2023.1186173

1 day, the score of these small structures may rise significantly, and they would overtake the three leading candidates (Araguainha, Ries, and Vredefort). Conversely, had the limit been extended to 3 days or more, Meteor Crater, Talemzane, and Steinheim would receive the lowest scores. The scores at the largest sites that are least accessible (Northern Canada) would then be augmented, leaving practically all candidate sites with a similar, high mark.

4.2.3 Geological features and lithologies

Geological features and lithologies are divided into impact features and lithologies (IFL) and target features and lithologies (TFL). The results for the different factors in both categories are given in Table 2.

4.2.3.1 Impact features and lithologies

The first four IFL factors listed in Table 2 characterize young and fresh impact structures (Meteor Crater, Ries, Steinheim, and Talemzane). All others receive a 0 mark for these four factors. Regarding the first factor, ejecta blanket, it has been eroded at Steinheim (mark 0). Meteor Crater is younger and less eroded than Ries, yet Ries is larger, and the amount and variety of ejecta is large. Both Meteor Crater and Ries, thus, are given the same intermediate mark of 2. Talemzane, which is more eroded, is marked 1. The same marks are given to these structures for the "ejecta block" factor, an impact feature that was noticed, visited, and described on the Moon by Apollo astronauts. Although the ejecta blanket is no longer exposed at Steinheim, some ejecta blocks are still present, giving it a 1. Overturned flap is an important, distinctive impact feature exposed in the inner walls near the top of the rim and immediately beyond into the ejecta blanket. No other geological process (volcano, intrusion, diapir) produces such a feature. This feature is well exposed at Meteor Crater (mark 2; see Kenkmann et al., 2014) and, to a lesser extent, at Talemzane (mark 1). Finally, bulking, veining, fracturing, slumping, and other geological features in the walls of impact craters are only well exposed at Meteor Crater, which gets a 3. At Talemzane, these features are partially preserved (mark 1), yet they no longer exist at Ries and Steinheim, both of which get a 0 for IFL-4.

The next 5 factors (IFL-5 to IFL-10, Table 2) deal with impact features or lithologies related to the crater fill. IFL-5 is marked 0 at Meteor Crater because the structure is still young and the crater depression is covered with alluvium and debris off the crater walls. However, the crater deposit has been accessed via drill cores. Vredefort also gets a mark of 0, but for the opposite reason. It is too eroded, below the crater floor. Although Steinheim, which is a small but complex impact structure, is more eroded than Meteor Crater, and although the floor of the crater emerges at the center of the structure, the crater fill deposit situation is similar to that at Meteor Crater. Crater fill deposit is buried in the crater moat region and is only known from drilling. Thus, it is a 0 for IFL-5, and for all the other factors related to the crater fill (IFL-6 to IFL-10). At Talemzane, the crater is more eroded than at Meteor Crater and some of the crater fill deposit is exposed at the foot of the wall. This structure receives a mark of 1 for IFL-5. At Sudbury, only a part of the crater fill deposit is exposed. It is also rated 1. Clearwater West and Mistastin are much younger and better preserved. Although partly covered by water, they locally display good exposures of crater fill deposits resulting in a mark of 2. At Ries, some crater fill deposit is exposed in quarries but most is covered by up to several hundred meters of crater lake deposits. This scenario results in a mark of 1 for IFL-5. At Araguainha, there is no sediment and no water masking the crater deposit that is moderately well preserved and quite well exposed along road sections. It is, thus, given a mark of 2. Rochechouart is more eroded, yet, the crater fill record is remarkable and diverse. It therefore also deserves a 2. Eventually, Haughton gets the highest mark (3) because the crater fill deposits are extensively exposed as a result of widespread and deep Arctic erosion and weathering.

Polymict lithic impact breccia (IFL-6) is best exposed at Ries, where it is represented by "Bunte Breccia," and at Rochechouart, where this impact breccia type forms the largest exposures of the crater fill. For that, both structures score 3. Polymict lithic breccia is not represented at Vredefort (0), but there is some at Clearwater West, Haughton, Meteor Crater, and Mistastin that all get a 1. Polymict lithic impact breccia is relatively well exposed at Araguainha, which scores a 2.

Suevite is best exposed at Ries, which is the reference locality for this rock type. It gets the highest mark for IFL-7. Haughton also gets a 3. The virtually continuous ~60 km^2 deposit covering the central area of the structure matches the field characteristics of suevite, although the matrix may have been initially partially molten (carbonatitic melt). Suevite is also relatively well exposed at Araguainha and Rochechouart, giving them a 2. There are some occurrences at West Clearwater and Mistastin, for a 1. The Onaping Formation exposures at the center of the Sudbury structure are extensive, but this material is debated as possibly having been reworked. Thus, conservatively, we are rating this deposit a 1. Vredefort lacks any suevite.

Rochechouart is the only selected impact site to expose very fine-grained material in the field bearing impact spherules, denominated by Lambert (2010) as impactoclastite. This phase has been interpreted as the product of condensation and settling of fines from the impact plume. Exposure in the field is scarce, so this occurrence is ranked 1.

Among the typical crater fill features of some large impact structures, one counts an impact melt layer. The best and most prominent case of impact melt rock development is at Sudbury, where the Sudbury Igneous Complex constitutes the largest exposed terrestrial impact melt sheet. Sudbury, thus, gets a mark of 3. Clearwater West and Mistastin come next where an impact melt sheet is locally well exposed (for a mark of 2). Some occurrence of an impact melt sheet is exposed at Rochechouart (gets a mark of 1). Araguainha, Haughton, and Ries, as well as the smaller craters, do not feature massive impact melt sheet developments and thus all get a 0.

Sudbury also gets the highest mark for impact melt rock (IFL-10), together with Mistastin and West Clearwater, where impact melt rocks are well represented. Then come Araguainha and Rochechouart, where the occurrences are more limited and, yet, expose a range of textures. They both get a mark of 2. Despite the deep level of erosion, impact melt rocks are observed in the central uplift structure at Vredefort in the form of a series of kilometer-long and up to 50-m-wide dikes. This prominent exposure is also rated 2. Impact melt rock is poorly represented at Ries and Talemzane that thus get a 1. It is absent elsewhere.

The IFL-11 to IFL-18 factors characterize the IFL related to the autochthonous and para-autochthonous material below and around the crater. At Meteor Crater, none of these features and lithologies are exposed. The crater is too fresh. A minimum of erosion is required to uncover these aspects. The contact between the crater fill deposit and autochthonous and para-autochthonous material below (referred to as basement in the following text) is of particular interest for the understanding of impact cratering mechanics. It is well exposed over a large zone at Rochechouart, resulting in a mark of 3 for IFL-11. It is also relatively well exposed at Araguainha that deserves a 2. At Clearwater West, Mistastin, Steinheim, and Sudbury, this contact is only locally exposed. They score 1. It is absent from the other structures (Table 2).

IFL-12 characterizes the exposure of the basement below the crater. Vredefort, where essentially only a deep level in the basement is exposed in the core of the central uplift, and Rochechouart, where the basement is widely exposed due to the abundant river drainage cutting through the crater fill deposit, get the highest mark of 3. At Araguainha, basement exposure is significant (mark 2), and at Clearwater West, Steinheim, and Sudbury, it is more limited (mark 1). At the other sites, the basement is not exposed.

A central uplift is a prominent feature characterizing large, complex impact structures. It can be expressed directly in the topography and indirectly (e.g., through localized stratigraphic uplift) in the geology. The readjustment of the basement during the modification stage of large impact events translates into large-scale deformation of the target rocks below the crater. IFL-13 relates to these features. They are particularly well exposed at Vredefort (getting a 3) and at Araguainha (also getting a 3), and to a lesser extent at Clearwater West, Mistastin, and Steinheim (scoring a 2). Some structural evidence of the central uplift is also visible in the field at Haughton and Rochechouart (getting a 1) but not at the other sites.

Related to the modification stage during large impact, the occurrence of large, displaced blocks (more than several meters to several hundred meters) in the target below the crater is best exposed at Ries, giving this structure a 3 for IFL-14. Some, up to hundreds-of-meters-sized megablocks, are exposed at Araguainha and Mistastin (mark 2). Some can also be seen at Clearwater West, Haughton, Rochechouart, and Steinheim for a mark of 1. Megablocks are absent from the other sites.

Monomict breccia may be a characteristic impact lithology below the crater floor at large impact structures. The highest mark for IFL-15 goes to Rochechouart where monomict breccias are relatively well exposed (mark 2). The other sites, but not Meteor Crater and Sudbury, locally display such a lithology that gives them a 1 in Table 2. At Araguainha, monomict breccias were mapped extensively by Von Engelhardt et al. (1992) but have since been shown to represent only locally brecciated basement of the Cuiabá Group.

Shatter cones represent the only macroscopic/mesoscopic criterion diagnostic of impact structures. All the aforementioned impact lithologies have counterparts produced by natural phenomena, with similar texture and appearance (such as volcanic/tectonic/sedimentary breccias, lava similar to impact melt rock, and others). Then, only detailed investigation at the microscopic scale and/or chemical analysis, both of which normally cannot be realized in the field, enable the identification of other characteristic shock features or traces of a meteoritic projectile. Shatter cones represent the only shock metamorphic feature recognizable in the field, or even in drill core. It is, thus, of high importance for astronauts and/or robots doing planetary fieldwork, to recognize such features, record and even understand their geological context, and distinguish shatter cones from similar features produced by other processes (e.g., wind ablation features, percussion marks, slickensides, or metamorphic foliation; see Baratoux and Reimold, 2016).

Shatter cones are very well exposed at Araguainha, Steinheim, Sudbury, and Vredefort that all get a 3 for IFL-16. They are relatively well exposed at Haughton and Rochechouart (which get a 2). Some have been described from Clearwater West, Mistastin, and Ries, giving them a 1, but none have been recorded from Meteor Crater or Talemzane (0).

Breccia dikes and veins are relatively common in the basement at Rochechouart and Talemzane, giving them a 2 for IFL-17. Some are observed at Araguainha, West Clearwater, Mistastin, and Vredefort, scoring a 1; none are exposed at the other sites that score a 0.

IFL-18 refers to pseudotachylite (friction melt) and pseudotachylitic breccia (other melt rock types in veins or dike form as discussed by Reimold, 2005; Reimold et al., 2016; and Spray and Biren, 2021). The type locality for pseudotachylite has been the Vredefort structure (Shand, 1916) but that was prior to the recognition that several types/generations of such breccia can be generated or exhumed in the impact process. The term pseudotachylite is exclusively reserved in structural geology for friction-generated melt rock. A specific type of such veining known as "shock veins" is generated during shock compression–decompression during the earliest stages of impact cratering, and typically such veinlets carry high-pressure polymorphs of minerals. Pseudotachylite and pseudotachylitic breccia are particularly well exposed at Vredefort and Sudbury (Sudbury Breccia) that score a 3. Occurrences are also known from Araguainha (mark 2), somewhat less from Mistastin and Rochechouart, giving these structures a mark of 1. Other sites score a 0.

Finally, IFL-19 and IFL-20 relate to features that are directly or indirectly linked to impact but which may be of significant interest while exploring impact structures on planetary surfaces. IFL-19 deals with the occurrence of valuable impact and/or post-impact mineralization. The interest for IFL-20 relates to the fundamental question of the emergence and sustainability of life, in the context of the ultra-dynamic impact process. These features are essentially linked with impact-triggered hydrothermalism. For these features, the score is 1 when evidence for late-stage (in the cratering sequence) hydrothermal mineralization can be observed in the field, and it is 0 when not. As far as impact and/or post-impact ore mineralization (IFL-19) is concerned, only Vredefort and Sudbury are notable for related mining provinces, thus getting a 1. Impact and/or post-impact hydrothermal features are observed in the field at Araguainha, Haughton, Ries, Rochechouart, Steinheim, and Sudbury. These structures get a 1 for IFL-20.

The total values for the 20 IFL factors (Table 2) are plotted in diminishing order in proportion of the best score in Figure 9D. There is a relatively large scatter of results. Mistastin and Ries score the same. Rochechouart gets the highest score, reflecting the wide variety of IFL exposed. Here, only four of the IFL factors score 0,

all corresponding to the features and lithologies typical for young and fresh impact sites. The 14 IFL factors symptomatic of impact crater fill and for the target are listed as IFL-5 to IFL-18 in Table 2. At Ries, 7 out of these 14 are factors can not be credited, and Ries, thus, scores in fourth place overall, together with Mistastin, with 37% below Rochechouart (Figure 9D).

Araguainha gets the second-best overall mark for IFL, only 11% below Rochechouart. As the latter, it scores 0 for IFL-1 to IFL-4, but then displays the third largest variety of IFL other than characteristics typical of young and fresh impact sites. The impactoclastite and impact melt layer are not represented. Sudbury suffers from the same limitations as Araguainha and gets the third best score for IFL, 15% below Araguainha (Figure 9D). Sudbury and Vredefort get the highest mark (3) for four IFL factors and are served by the extra points attributed for impact/post-impact economic mineralization and hydrothermalism. They get a relatively high overall score for IFL, with Sudbury ranking even above Mistastin and Ries (Figure 9D). Eventually, Vredefort scores 14% below Mistastin and Ries. Clearwater West is 3% above Vredefort, and Haughton 8% below Vredefort.

Although receiving marks for the first four IFL factors, the three smallest and youngest structures, Steinheim, Meteor Crater, and Talemzane, get the lowest totals for IFL. They rank 60% below the overall mark for Rochechouart.

4.2.3.2 Target features and lithologies

The lower part of Table 2 summarizes the results for TFL, which characterize the tuition value of the various sites (up to 20 km away from the structure) for recognizing country rocks and general regional geological processes. TFL-1 and TFL-2 relate to the two main categories of sedimentary rocks, limestone/dolomite grouped under the label "carbonates," and arenites (mainly sandstone). TFL-3 represents all other sedimentary rocks. Carbonates are very well exposed at Haughton, Meteor Crater, Ries, Talemzane, and in the wider Vredefort Structure, giving them a 3 for TFL-1. They are also relatively well exposed at Steinheim scoring 2. There is evidence of carbonate involvement with the target at Araguainha, Clearwater West, and at the periphery of Rochechouart, and all of these get a 1. Mistastin and Sudbury obtain a 0 value for TFL-1.

Sandstones are well exposed at Araguainha and Ries, for which the TFL-2 is 3. Meteor Crater exposes an entire sandstone formation sequence, also for a 3. There is evidence of sandstone at Haughton, Steinheim, Sudbury, and at the periphery of Rochechouart, giving them a 1. Sandstones or arenites are not exposed at Clearwater West, Mistastin, and Talemzane, nor at Vredefort where instead metamorphic equivalents occur (see below), which results in a 0 mark for TFL-2. The same applies to other sedimentary rocks, especially shales that are abundant at Vredefort, but are not sedimentary rocks *sensu stricto* (TFL-3 is then 0). Other sedimentary rocks, however not very prominent, can be observed in the field at Araguainha, Haughton, Mistastin, Ries, Steinheim, and Sudbury, giving these structures a 1 for TFL-3. They are absent at the other sites, thus scoring a 0.

TFL-4 to TFL-7 consider the presence of magmatic features in the field. They are not exposed at Haughton, Meteor Crater, Ries, Steinheim, Sudbury, and Talemzane, all of which get a 0 for these four factors. Granites and other felsic granitoids are well represented in the field at Araguainha, Rochechouart, Vredefort, and Sudbury, which get a 3 for TFL-4. Some magmatic rocks of intermediate composition (diorites) occur at Rochechouart, which gets a 1 for TFL-5. They are well represented at Mistastin (anorthosite) for a 3. They are absent at the other sites. Mafic intrusives are prominent in the Vredefort structure resulting in a 3 for TFL-6. Some are also exposed at Clearwater West (dolerites) and at Rochechouart (lamprophyres). Both these structures obtain a 1, whereas TFL-6 is 0 for all other structures. Exposures of primary intrusive ultramafic rocks (such as peridotites) are not present at any of these sites.

TFL-8 to TFL-11 relate to metamorphic lithologies. None are exposed at Haughton, Meteor Crater, Steinheim, and Talemzane and all receive 0 marks. Felsic metamorphic rocks (schist, mica-schist, gneiss, leptynite, meta-arenites, etc.) are very well exposed at Clearwater West, Mistastin, Rochechouart, Sudbury, and Vredefort, all of which score 3 for TFL-8. Some are exposed at Ries and at Araguainha (phyllite, schist, meta-arenite), giving them a 1. Metamorphic rocks of intermediate composition are well exposed at Sudbury and Vredefort (epidiorite). They get a 3 for IFL-9. Schists of intermediate composition are relatively well exposed at Araguainha, which gets a 2 for TFL-9. Intermediate metamorphic rocks are not exposed at Clearwater West, which gets a score of 0 for TFL-9.

There are some mafic rocks known from the Clearwater structures, Rochechouart (amphibolite), and various Variscan metamorphic gneiss types from the Ries. The crystalline basement core at Vredefort contains ample mafic gneiss. The target at Sudbury also comprises some mafic metamorphic rocks. All these structures score a 1 for TFL-10. Finally, ultramafic metamorphic rocks are only exposed at Rochechouart (serpentinite) and Sudbury (Sublayer material), and score a 1 for TFL-11.

The total TFL marks (Table 2) are plotted in diminishing order, in proportion of the best score, in Figure 9E. The scatter is large, even larger than for the total IFL marks (Figure 9D). Vredefort gets the highest score, as it displays a grand variety of TFL, scoring in 6 of the 11 categories. Yet, Rochechouart, with the second-best overall score at 19% below Vredefort, scores in nine categories. Vredefort is distinguished by the quality of exposures. It gets the highest scores (3) in four of the TFL factors, which includes one in each of the three major categories of rock types, sedimentary, igneous, and metamorphic. Rochechouart does cover a larger variety of major rock types but the quality of exposure is less than it is at Vredefort. Rochechouart only gets the highest mark (3) for 2 of the TFL (felsic intrusive and felsic metamorphic rocks) categories. The third-best site for TFL is Araguainha, at 31% below Vredefort, followed closely by Ries and Sudbury, both scoring 6% below Araguainha (Figure 9E). These three structures get the highest marks for two of the TFL factors, but Araguainha offers a larger diversity. In the sixth position is Mistastin, 13% below Ries and Sudbury, followed by Clearwater West, 12% below Mistastin. Haughton and Meteor Crater score 7% below Clearwater West. As observed for the IFL, the lowest totals for TFL are obtained by the smallest impact structures (Meteor Crater, Steinheim, and Talemzane).

4.2.3.3 Aggregate result: Geological Features and Lithologies

The GFL factors correspond to the sum of the marks obtained for 20 IFL and 11 TFL factors. Figure 10A shows the results in tabular (on the left) and graphic (on the right) modes. The aggregate GFL

A

	IFL+TFL	GFL
Araguainha	35	3.5
Clearwater West	22	2.2
Haughton Dome	18	1.8
Meteor Crater	15	1.5
Mistastin Lake	27	2.7
Ries	29	2.9
Rochechouart	40	4
Steinheim	15	1.5
Sudbury	30	3
Talemzane	13	1.3
Vredefort	31	3.1

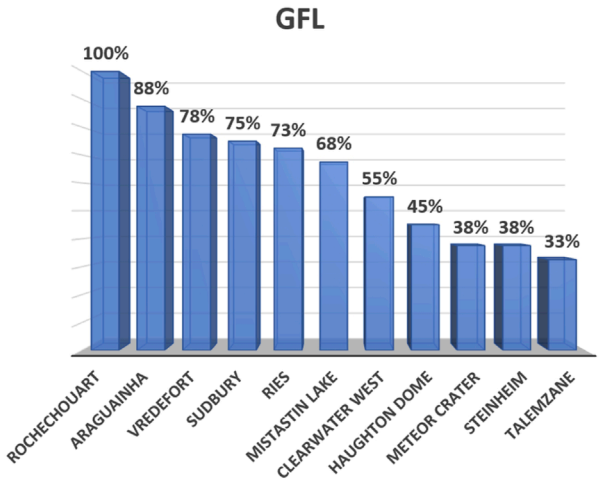

B

	CP	OS	GFL	GC
Araguainha	2.4	4	3.5	3.92
Clearwater West	2.4	2.7	2.3	2.98
Haughton Dome	2.4	2	1.8	2.51
Meteor Crater	4	3.3	1.5	3.57
Mistastin Lake	2.4	2.7	2.4	3.02
Ries	3.2	4	2.7	4
Rochechouart	1.6	2.7	4	3.34
Steinheim	2.4	2.7	1.5	2.65
Sudbury	1.6	3.3	3	3.21
Talemzane	3.2	3.3	1.3	3.16
Vredefort	0.8	4	3.1	3.19

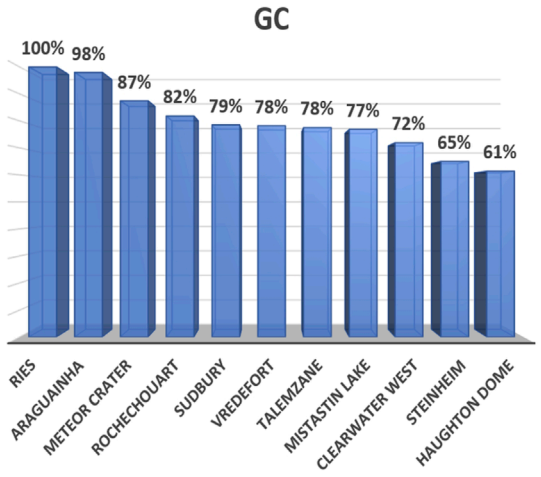

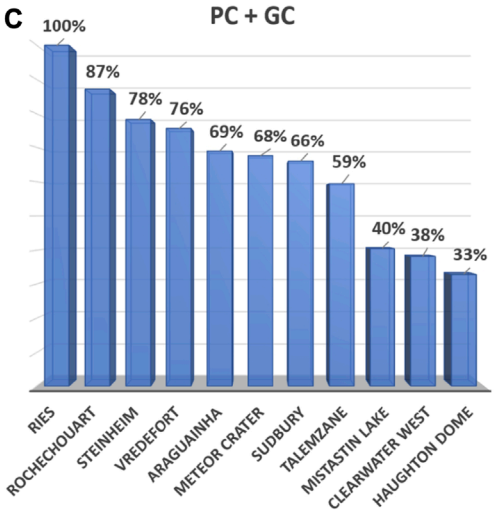

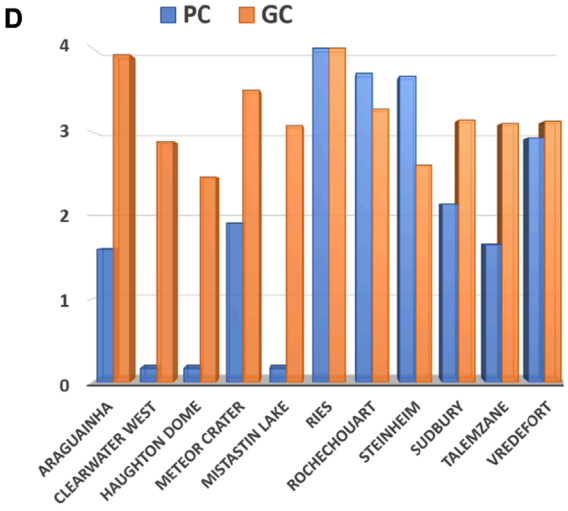

FIGURE 10
(A) Geological Features and Lithology (GFL) marks. Left: total of the Impact Features and Lithologies (IFL) marks and Target Features and Lithologies (TFL) marks scaled to 4 (GFL column) (values from Table 2). Right: results for the geological features and lithologies factor plotted in decreasing order and with values in proportion to the best score. **(B)** Geological Criteria (GC) marks. Left: marks scaled to 4, for the crater preservation (CP) factor; CS, cost factor; OS, outcrop situation factor; GFL, geology features and lithologies factor. GC: overall Geological Criteria marks corresponding to the total obtained for each site for the three geology factors, normalized to the highest scores and scaled to 4. Right: ranking of the GC results in proportions of the best score. **(C)** Ranking of the overall results in proportions of the best score. **(D)** Comparison of the marks obtained for the Practical Criteria (PC) and GC.

mark corresponds to the total IFL + TFL marks—scaled to 4. IFL and TFL do not contribute equally to the GFL result, as the number of IFL factors considered is larger (1.8 times larger) than the TFL factors. Rochechouart takes the lead for the overall GFL marks. The ranking reflects the trend noticed for both the IFL and TFL factors. The lowest scores go to the three youngest and smallest structures (Meteor Crater, Steinheim, and Talemzane), at less than 40% of Rochechouart.

Next are the overall GFL values for Ries, Mistastin, Clearwater West, and Haughton, which are mid-sized and still relatively young and fresh, and then for Vredefort and Sudbury, the very old and very large candidates. The best GFL scores are obtained by Rochechouart and Araguainha, both medium sized and moderate in age. This illustrates the importance of erosion. Erosion is required to expose IFL, but it may also remove important features. Thus, the right balance between too much erosion and not enough has to be met. And this is precisely the case for Araguainha and Rochechouart. While crater morphology is reduced or lost, much of the IFL is still preserved. Furthermore, erosion has cut across the crater fill deposit and locally exposed the basement and related IFL, which include shock damage and impactite pods and dikes produced or emplaced below the crater floor. This is most obvious at Rochechouart where the contact between the crater fill deposit and basement is largely exposed thanks to river drainage cutting into the impact deposit. At Araguainha, extensive road works have recently generated new insights into the lower crater fill deposit, crater floor, and basement. The variety of exposed features and lithologies tends to increase with the size of the structures, as we consider not only IFL but also TFL. The latter is responsible for a good overall GFL score for Vredefort (78%; Figure 10A).

4.2.4 Overall result for geological criteria

The overall GC mark is obtained by combining, with an equal weight, the three geology factors (CP, OS, and GFL). The totals obtained for the different sites for the three geology factors are normalized to the highest scores and scaled to 4. The resulting scores are given in Figure 10B, in tabular (on the left) and graphic (on the right) modes, as proportions of the highest score. The range of values is relatively small, at less than 40% variance between the highest and lowest results (Figure 10B).

Two sites are leading, with one not coming as a surprise—the Ries Crater. It is the best known and most extensively studied impact site in the terrestrial impact record. However, the co-leader, only 2% below Ries, is, quite unexpectedly, the Araguainha structure in Brazil. Araguainha falls into the same size range (moderately sized impact structures) as Ries and is of the same crater type (complex impact crater formed in a mixed sedimentary/crystalline target; comparison provided in Table 1). The Araguainha impact is, however, significantly older and its structure is accordingly not as well preserved as the Ries. Thus, these two candidates have different scores for the CP factor. Their scores for the OS are the same (Figure 10B). There is the larger range of GFL at Araguainha, which compensates for the lesser state of preservation and allows Ries and Araguainha to end with almost the same final score. Had the CP factor been further constrained with the help of other criteria such as topographic expression of the crater in the field, Ries might take a clearer lead over Araguainha.

Next in the GC record comes Meteor Crater (Figure 10B), scoring high at 87% of the leaders' values. This position contrasts with the low score obtained for the geology features and lithologies factor (35% below Ries—Figure 10A) and clearly reflects the relative weighting given to OS and CP, both to the advantage of the young and fresh craters in the desert terrain with respect to the geology features and lithologies factor. The GC for Rochechouart score 5% below Meteor Crater, which is followed by Sudbury, Vredefort, and Talemzane that are 4%–5% below Rochechouart (Figure 10B). Mistastin and Clearwater West are 4%–5% below Talemzane, and Steinheim and Haughton conclude this series. Notably, even these two candidates still score relatively high, only 35% and 39% below the leaders.

4.3 Overall: final results

Based on the criteria and methodology proposed for this analysis, the suitability of the selected terrestrial impact sites as field analogs for extraterrestrial fieldwork on planetary surfaces is given by the sum of the marks for the PC and GC. These results are shown in a single score graph in Figure 10C. Ries clearly deserves the highest overall mark. It consistently receives good marks for all factors and is ranked first for both the PC and GC (Figure 10D). Ries is the best candidate in terms of time efficiency and OS. However, considering solely the GFL, Ries does not rank the highest—although still with a relatively high mark only 28% below Rochechouart that leads the GFL classification (Figure 10A).

Rochechouart is the second-best candidate site, only 13% below Ries (Figure 10C). The spread of Rochechouart's individual marks is wider than those for Ries, with a relatively low mark for CP and medium marks for OS. This lowers its GC mark when compared to Ries (Figure 10B), and Rochechouart also has low marks for the OLF, lowering its PC score when compared to Ries (Figure 9A, Figure 10D). By contrast, Rochechouart has the top ranking for time, benefits, and geological features and lithology factors that achieve the overall high score. Next are Steinheim and Vredefort at 9% and 11% below Rochechouart, respectively (Figure 10C). The higher scores of Steinheim when compared to Vredefort for the PC compensates for its lower mark for the GC (Figure 9A; 10D). Next comes a group of three sites, with Araguainha, Meteor Crater, and Sudbury still scoring high at 31%–34% below the leader, and 7%–10% below Vredefort (Figure 10C). Araguainha is penalized by its low score for the PC and bolstered by an excellent GC ranking. For Meteor Crater and Sudbury geology scores are less, but their practical score is higher (Figure 9A, Figure 10D). Talemzane, 7% below Sudbury and 41% below the leader, finishes with a relatively good score (Figure 10C) because of a good geology score (Figure 9A, Figure 10D), and served by excellent CP and OS marks (Figures 9B, C).

The three Northern Canada sites end close to each other, yet with significantly lower overall scores than their competitors. They fall 60%–67% below Ries and 19%–24% below Talemzane (Figure 10C). This is mainly due to their very poor performance regarding the PC (Figure 10C), and they do not score high for geology either. At Clearwater West and Mistastin, the lakes prevent exposition of a larger array of geology features and lithologies, while at Haughton,

this is prevented by limited erosion and the large coverage with melt-bearing polymict breccia.

5 Conclusion

We have discussed that there will be strong, ongoing requirements for terrestrial field training at impact structures, in view of future planetary expeditions by astronauts or robots. Based on a varied set of criteria, a selection of terrestrial impact analog sites has been evaluated to set a benchmark example of methodology for expedition planners. The approach combines the widest variety of criteria marking the practical value and the geological value of the selected sites. We have given an equal value to the PC and GC, and the overall result identifies and ranks the sites accordingly. Owing to the variety of size, age, and morphological types of impact structures, the terrestrial impact record does not offer an individual site that can get the highest mark for each criterion. This is especially true for the GC, where strongly competing factors are involved. The small-sized impact structures do not develop the full range of IFL, and all of those do not occur at the same level within an impact structure [some are only found at the upper level (ejecta, rim) and some at depth (shatter cones, pseudotachylitic breccias)]. Erosion is at play and may remove interesting features, while exposing others. In addition, the nature of the target, the overall terrane environment in which the sites are located, and the size of the structure interact with the rate of erosion, which is itself related to the location, the paleoclimatic history, and more generally, the geological history involved at any given site.

Nevertheless, the proposed methodology allows to distinguish the sites that are globally the best suited in terms of our thought experiment. Ries is the overall winner. It receives the highest score for both the PC and GC. Notably, Ries was already visited by Apollo astronauts in 1970 and by ESA astronauts in 2022 (Mangold et al., 2022; Sauro et al., 2022).

Ries is followed by Rochechouart with good accessibility and practical benefits, and by a wide range of IFL (despite its significant erosion level). Meteor Crater and Sudbury, which have already served as training sites for astronauts since the Apollo missions score almost the same in the sixth and seventh positions. At equal distance from Rochechouart and Meteor Crater (or in terms of ranking between Rochechouart and Meteor Crater), Steinheim and Vredefort score almost the same, lying in third and fourth positions. Then, Araguainha and Meteor Crater almost score the same with a small advantage to the Brazilian impact structure. At the end are the three Northern Canadian impact structures, Clearwater West, Haughton, and Mistastin, which are used as training sites by the Canadian Space Agency. The lack of accessibility on all grounds (access to the structure and then access to the outcrops once on site) is even compared to more suitable sites in Africa and South America and are largely responsible for these low scores. The geology is relatively well exposed in Northern Canada but does not manage to compensate. Two of the structures (Clearwater West and Mistastin) are largely underwater, unlike all the other selected sites.

The study shows that the overall access time and cost for getting to the three European sites are most competitive when coming from China or Japan. Even when starting in Canada or the United States, they are not very different from those for Meteor Crater and Sudbury, and do not compare to the three Northern Canada sites which require much more time at a much higher cost.

In the context of this specific application, and considering

- the scores of the three sites in Western Europe (that received the highest marks);
- their complementarity (the TFL are complementary; the topography and impact ejecta that are missing at Rochechouart are well exposed at Ries and Steinheim; inversely, the crater fill deposits, crater floor, and target beneath the crater that are not exposed at Ries and Steinheim can be studied at Rochechouart);
- their accessibility and practical benefits; and
- their relative proximity to each other (Ries and Rochechouart are a day's drive apart and Steinheim is on the way),

we recommend a "joint expedition" to these three impact sites, and a "composite venue" for administration and other logistics. Such a site office could serve all agencies concerned with the exploration and exploitation of impact related features on planetary surfaces.

Finally, our experiment may be considered a "template" for comparison of our candidate structures with other sites or for other expedition foci. However, this is not to say that our approach alone may be the best in each and every case. For instance, some factors could be added, such as the CO_2 imprint of accessing impact sites (which would penalize the three Northern Canada sites even more and reinforce the leading position of Ries and Rochechouart that are both easily accessible by train). Factors could also be affected by a coefficient according to specific requirements or priorities, possibly modifying the overall ranking. We do hope, however, the present work will be useful and that these ideas will stimulate further analysis.

Data availability statement

The original contributions presented in the study are included in the article/Supplementary Material; further inquiries can be directed to the corresponding author.

Author contributions

All authors listed have made a substantial, direct, and intellectual contribution to the work and approved it for publication.

Funding

The work of WUR was financed in part by the Coordenação de Aperfeiçoamento de Pessoal de Nível Superior, Brasil (CAPES); Finance Code 001.

Acknowledgments

The paper benefited from the help and support of many members of CIRIR. The authors especially thank Manfred

Gottwald, Yoann Quesnel, and Gisela Poesges for providing illustrative material. Philippe Lambert expresses his gratitude to the Community of Communities "Charente Limousine, the Community of Communities" "Porte-Océane du Limousin" and the board of administration of the CIRIR for their continuing support. Uwe Reimold is most grateful for the fruitful discussions about Araguainha with Natalia Hauser.

Conflict of interest

The authors declare that the research was conducted in the absence of any commercial or financial relationships that could be construed as a potential conflict of interest.

Publisher's note

Supplementary material

The Supplementary Material for this article can be found online at: https://www.frontiersin.org/articles/10.3389/fspas.2023.1186173/full#supplementary-material

References

Abramov, O., and Kring, D. A. (2004). Numerical modeling of an impact-induced hydrothermal system at the Sudbury crater. *J. Geophys. Res.* 109, E10007. doi:10.1029/2003JE002213

Allen, N. H., Nakajima, M., Wünnemann, K., Helhoski, S., and Trail, D. (2022). A revision of the formation conditions of the Vredefort crater. *J. Geophys. Res. Planets* 127, e2022JE007186. doi:10.1029/2022JE007186

Artemieva, N. A., Wünnemann, K., Krien, F., Reimold, W. U., and Stöffler, D. (2013). Ries crater and suevite revisited-observations and modeling Part II: modeling. *Model. Meteorit. Planet. Sci.* 48, 590–627. doi:10.1111/maps.12085

Baratoux, D., and Reimold, W. U. (2016). The current state of knowledge about shatter cones: introduction to the special issue. *Meteorit. Planet. Sci.* 51, 1389–1434. doi:10.1111/maps.12678

Barringer, D. M. (1910). *Meteor Crater (formerly called Coon Mountain or Coon Butte) in northern central Arizona*. Princeton, NJ, United States: National Academy of Sciences, Princeton University, 24.

Biren, M. B., van Soest, M. C., Wartho, J. A., Hodges, K. V., and Spray, J. G. (2016). Diachroneity of the Clearwater West and Clearwater East impact structures indicated by the (U–Th)/He dating method. *Earth Planet. Sci. Lett.* 453, 56–66. doi:10.1016/j.epsl.2016.07.053

Bischoff, L., and Oskierski, W. (1988). The surface structure of the Haughton impact crater, Devon Island, Canada. *Meteorit* 23, 209–220. doi:10.1111/j.1945-5100.1988.tb01283.x

Brustel, C., Flahaut, J., Hauber, E., Fueten, F., Quantin, C., Stesky, R., et al. (2017). Valles Marineris tectonic and volcanic history inferred from dikes in eastern Coprates Chasma. *J. Geophys. Res. Planets* 122, 1353–1371. doi:10.1002/2016JE005231

Buchner, E., Sach, V. J., and Schmieder, M. (2022). Event- and biostratigraphic evidence for two independent Ries and Steinheim asteroid impacts in the Middle Miocene. *Sci. Rep.* 12, 18603. doi:10.1038/s41598-022-21409-8

Busson, G. (1970). Le Mésozoïque saharien. Essai de synthèse des données de sondages algéro-tunisiens. *CNRS-CRZA, S. Géol , n°* 11, 788.

Chabou, M. C. (2019). "Meteorite impact structures in the arab world: an overview," in *The geology of the arab world—an overview*. Editors A. Bendaoud, Z. Hamimi, M. Hamoudi, S. Djemai, and B. Zoheir (Cham, Germany: Springer), 455–506. doi:10.1007/978-3-319-96794-3_13

Chao, E. C. T., Shoemaker, E. M., and Madsen, B. M. (1960). First natural occurrence of coesite. *Science* 132 (3421), 220–222. doi:10.1126/science.132.3421.220

Cockell, C. S., and Lee, P. (2002). The biology of impact craters – a review. *Biol. Rev.* 77, 279–310. doi:10.1017/s146479310100584x

Cockell, C. S., Osinski, G. S., and Lee, P. (2003). The impact crater as a habitat: effects of impact processing of target materials. *Astrobiol* 3, 181–191. doi:10.1089/153110703321632507

Crósta, A. P., Reimold, W. U., Hauser, N., Vasconcelos, M. A. C., Mazivieiro Velzic, M., Oliveira, G. J., et al. (2019). Impact cratering: the south American record – Part 1. *Geochem. - Chem. Erde* 79, 1–61. doi:10.1016/j.chemer.2018.06.001

Dence, M. R. (1964). A comparative structural and petrographic study of probable Canadian meteorite craters. *Meteoritics* 2 (3), 249–270. doi:10.1111/j.1945-5100.1964.tb01432.x

Dence, M. R., Innes, M. J. S., and Beals, C. S. (1965). On the probable meteorite origin of the clearwater lakes, Quebec. *J. R. Astronomical Soc. Can.* 59, 1–213.

Dietz, R. S. (1959). Shatter cones in cryptoexplosion structures (Meteorite impact?). *J. Geol.* 67, 496–505. doi:10.1086/626603

Fabre, J. (1974). Introduction à la géologie du Sahara algérien et des régions voisines: la couverture phanérozoïque. *SNED, Alger* 1, 422.

Faure, M., Lardeaux, J.-M., and Ledru, P. (2009). A review of the pre-Permian geology of the Variscan French Massif Central. *C.R. Geosci.* 341, 202–213. doi:10.1016/j.crte.2008.12.001

French, B. M. (1998). *Traces of catastrophe: A handbook of shock-metamorphic effects in terrestrial impact structures. LPI contribution*. Houston, Texas, United States: Lunar and Planetary Institute, 120.

French, B. M., and Koeberl, C. (2010). The convincing identification of terrestrial meteorite impact structures: what works, what doesn't and why. *Earth Sci. Rev.* 98, 123–170. doi:10.1016/j.earscirev.2009.10.009

Frimmel, H. E. (2019). "The Witwatersrand Basin and its gold deposits," in *The Archaean Geology of the Kaapvaal Craton, southern Africa. Regional geology reviews*. Editors A. Kröner, and A. Hofmann (Cham, Germany: Springer), 255–275. doi:10.1007/978-3-319-78652-0_10

Gibson, R. L., and Reimold, W. U. (2008). *The Geology of the Vredefort Impact Structure*. Pretoria, South Africa: Council for Geoscience, 181.

Gottwald, M., Kenkmann, T., and Reimold, W. U. (2020). *Terrestrial impact structures, the TanDEM-X atlas, Part 1 and 2*. München, Germany: Verlag Dr. Friedrich Pfeil, 608.

Grieve, R. A. F. (2006). *Impact structures in Canada*. St. Johns, Canada: Geological Association of Canada, Memorial Univ. of Newfoundland, 210.

Grieve, R. A. F., Reimold, W. U., Morgan, J., Riller, U., and Pilkington, M. (2008). Observations and interpretations at Vredefort, Sudbury, and Chicxulub: towards an empirical model of terrestrial impact basin formation. *Meteorit. Planet. Sci.* 43, 855–882. doi:10.1111/j.1945-5100.2008.tb01086.x

Hauser, N., Reimold, W. U., Cavosie, A. J., Crósta, A. P., Schwarz, W. H., Trieloff, M., et al. (2019). Linking shock textures revealed by BSE, CL, and EBSD with U-Pb data (LA-ICP-MS and SIMS) from zircon from the Araguainha impact structure, Brazil. *Meteorit. Planet. Sci.* 54, 2286–2311. doi:10.1111/maps.13371

Huber, M. S., Koeberl, C., Smith, F. S., Glass, B. P., Mundil, R., and McDonald, I. (2009). Geochemistry of a confirmed Precambrian impact ejecta deposit: the grænsesø spherule layer, South Greenland. *Meteorit. Planet. Sci.* 54, 2254–2272. doi:10.1111/maps.13271

Huber, M. S., Črne, A. E., McDonald, I., Hecht, L., Melezhik, V. A., and Koeberl, C. (2014). Impact spherules from Karelia, Russia: possible ejecta from the 2.02 Ga vredefort impact event. *Geology* 42, 375–378. doi:10.1130/g35231.1

Janssens, M. J., Hertogen, J., Takahashi, H., Anders, E., and Lambert, P. (1977). Rochechouart meteorite crater: identification of projectile. *J. Geophys. Res.* 82, 750–758. doi:10.1029/JB082i005p00750

Kamo, S. L., Reimold, W. U., Krogh, T. E., and Colliston, W. P. (1996). A 2.023 Ga age for the Vredefort impact event and a first report of shock metamorphosed zircons in pseudotachylitic breccias and Granophyre. *Earth Planet. Sci. Lett.* 144, 369–387. doi:10.1016/S0012-821X(96)00180-X

Kenkmann, T., Poelchau, M. H., and Wulf, G. (2014). Structural geology of impact craters. *J. Struct. Geol.* 62, 156–182. doi:10.1016/j.jsg.2014.01.015

Kenkmann, T. (2021). The terrestrial impact crater record: A statistical analysis of morphologies, structures, ages, lithologies, and more. *Meteorit. Planet. Sci.* 56, 1024–1070. doi:10.1111/maps.13657

Koeberl, C. (2014) "The geochemistry and cosmochemistry of impacts," in *Treatise on geochemistry*, Editor H. D. Holland, 2nd edition (Amsterdam, Netherlands, Elsevier Publishers), 73–118.

Kovaleva, E., Kusiak, M. A., Kenny, G. G., Whitehouse, M. J., Habler, G., Schreiber, A., et al. (2021). Nano-scale investigation of granular neoblastic zircon, Vredefort impact structure, South Africa: evidence for complete shock melting. *Earth Planet. Sci. Lett.* 565, 116948. doi:10.1016/j.epsl.2021.116948

Kraut, F., and French, B. M. (1971). The Rochechouart meteorite impact structure, France: preliminary geological results. *J. Geophys. Res.* 76, 5407–5413. doi:10.1029/jb076i023p05407

Kraut, F., Short, N., and French, B. M. (1969). Preliminary report on a probable meteorite impact structure near Chassenon. *Fr. Meteorit.* 4 (3), 190–191.

Kring, D. A. (1997). Air blast produced by the Meteor Crater impact event and a reconstruction of the affected environment. *Meteorit. Planet. Sci.* 32, 517–530. doi:10.1111/j.1945-5100.1997.tb01297.x

Kring, D. A. (2010). *What can astronauts learn from terrestrial impact craters for operations on the Moon and Mars? Noerdlinger Ries Crater workshop*. Houston, Texas, USA: Lunar and Planetary Institute.

Kring, D. A. (2017). *Guidebook to the geology of barringer meteorite crater*. Houston, Texas, USA: Lunar Planet. Inst., 272.

Lamali, A., Rochette, P., Merabet, N., Abtout, A., Maouche, S., Gattacceca, J., et al. (2016). Geophysical and magneto-structural study of the Maâdna structure (Talemzane, Algeria): insights on its age and origin. *Meteorit. Planet. Sci.* 51 (12), 2249–2273. doi:10.1111/maps.127152249

Lambert, P. (1975). Nickel enrichment of impact melt rocks from Rochechouart. Preliminary results and possibility of meteoritic contamination. *Meteoritics* 10, 433–436.

Lambert, P. (1977a). The Rochechouart crater: shock-zoning study. *Earth Planet. Sci. Lett.* 35, 258–268. doi:10.1016/0012-821x(77)90129-7

Lambert, P. (1977b). "Rochechouart impact crater: statistical geochemical investigations and meteoritic contamination," in *Impact and explosion cratering*. Editors D. J. Roddy, R. O. Pepin, and R. B. Merill (New York, NY, USA: Pergamon Press), 449–460.

Lambert, P. (2010). "Target and impact deposits at Rochechouart impact structure, France," in *Large Meteorite Impacts and Planetary Evolution IV*. Editors R. L. Gibson, and W. U. Reimold (Boulder, Colorado, United States: Geological Society of America), 509–541.

Lambert, P. (2019). "Current impacts stage of the CIRIR research and outreach at Rochechouart," in Large Meteorite Impacts and Planetary Evolution, VI, Brasilia, September/October 2019.

Lambert, P. (2022). The Rochechouart size, shape, age and environment. https://cirir-edu.org/wp-content/uploads/2022/06/ICF-CIRIR-2022-S1T14-Lambert.pdf.

Lambert, P., Alwmark, C., Baratoux, D., Bouley, S., Brack, A., Bruneton, P., et al. (2019). The Rochechouart 2017-cores rescaled: major features. Proceedings of the 50th Lunar and Planetary Science Conference, March 2019 The Woodlands, Texas, United States.pp.2083.

Lambert, P. (2023). The international congress–festival-CIRIR 2022 (ICF-CIRIR 2022), Rochechouart, France. *Meteorit. Planet. Sci.* 58 (2), 296–302. doi:10.1111/maps.13954

Leite, E. P., Lambert, J., Vasconcelos, M. A. R., Crósta, A. P., and Batezelli, A. (2022). Gamma-ray spectrometry of the araguainha impact structure, Brazil: additional insights into element mobilization due to hydrothermal alteration. *An. Acad. Bras. Cienc.* 94, e20210182 pp. doi:10.1590/0001-3765202220210182

Lightfoot, P. C. (2016). *Nickel sulfide ores and impact melts? Origin of the Sudbury igneous complex*. Amsterdam, Netherlands: Elsevier Publishers, 662.

Machado, R., Lana, C., Stevens, G., Filho, C. R. S., Reimold, W. U., and McDonald, I. (2009). Generation, mobilization, and crystallization of impact-induced alkali-rich melts in granitic target rocks: evidence from the Araguainha impact structure, central Brazil. *Geochim. Cosmochim. Acta* 73, 7183–7201. doi:10.1016/j.gca.2009.08.029

Mader, M. M., and Osinski, G. R. (2018). Impactites of the Mistastin Lake impact structure: insights into impact ejecta emplacement. *Meteorit. Planet. Sci.* 53, 2492–2518. doi:10.1111/maps.13173

Mangold, N., Sauro, F., Massironi, M., Pozzobon, R., Hiesinger, H., Cockell, C. S., et al. (2022). ESA PANGEA - training astronauts in field geology within UNESCO geoparks. https://cirir-edu.org/wp-content/uploads/2022/05/ICF-CIRIR-2022-S3T7-Mangold-et-al.pdf.

Marion, C. L., and Sylvester, P. J. (2010). Composition and heterogeneity of anorthositic impact melt at Mistastin Lake crater, Labrador. *Planet. Space Sci.* 58, 552–573. doi:10.1016/j.pss.2009.09.018

Naumov, M. V. (2002). "Impact-generated hydrothermal systems: data from Popigai, Kara, and Puchezh-Katunki impact structures," in *Impacts in Precambrian Shields*. Editors J. Plado, and L. J. Pesonen (New York, NY, USA: Springer), 117–171.

Nedjari, A., Ait Ouali, R., and Delfaud, J. (2002). Le Trias des bassins sahariens; mise au point et nouvelle approche. *Mém. Serv. Géol. Alg. n°* 1, 87–113.

Osinski, G. R. (2022). Preparing for Artemis: the importance of field geology training at impact analogue sites and the case for the Mistastin (Kamestastin) Lake impact structure. *Lunar Planet. Sci. Conf.* 51.

Osinski, G. R., and Spray, J. G. (2005). Tectonics of complex crater formation as revealed by the Haughton impact structure, Devon Island, Canadian High Arctic. *Meteorit. Planet. Sci.* 40, 1813–1834. doi:10.1111/j.1945-5100.2005.tb00148.x

Osinski, G. R., Lee, P., Spray, J. G., Parnell, J., Lim, D., Bunch, T. E., et al. (2005). Geological overview and cratering model for the Haughton impact structure, Devon Island, Canadian high arctic. *Meteorit. Planet. Sci.* 40, 1759–1776. doi:10.1111/j.1945-5100.2005.tb00145.x

Osinski, G. R., Grieve, R. A. F., and Spray, J. G. (2010). The nature of the groundmass of surficial suevite from the Ries impact structure, Germany, and constraints on its origin. *Meteorit. Planet. Sci.* 39, 1655–1683. doi:10.1111/j.1945-5100.2004.tb00065.x

Osinski, G. R., Tornabene, L. L., Banerjee, N. R., Cockell, C. S., Flemming, R., Izawa, M. R. M., et al. (2013). Impact-generated hydrothermal systems on Earth and Mars. *Icarus* 224, 347–363. doi:10.1016/j.icarus.2012.08.030

Osinski, G. R., Brunner, A., Collins, G. S., Cohen, B. A., Coulter, A., Elphic, R., et al. (2015). Revisiting the West Clearwater Lake impact structure, Canada, *Proceedings of the 46th Lunar and Planetary Science Conference*. The Woodlands, TX, USA

Osinski, G. R., Cockell, C. S., Pontefract, A., and Sapers, H. L. (2020). The role of meteorite impacts in the origin of life. *Astrobiology* 20 (9), 1121–1149. doi:10.1089/ast.2019.2203

Phinney, W. C. (2015). *Science training history of Apollo astronauts*. Washington, D.C., United States: NASA.

Plan, A., Kenny, G. G., Erickson, T. M., Lindgren, P., Alwmark, C., Holm-Alwmark, S., et al. (2022). Exceptional preservation of reidite in the Rochechouart impact structure, France: new insights into shock deformation and phase transition of zircon. *Meteorit. Planet. Sci.* 56, 1795–1828. doi:10.1111/maps.13723

Poelchau, M. H., Kenkmann, T., and Kring, D. A. (2009). Rim uplift and Crater shape in Meteor Crater: effects of target heterogeneities and trajectory obliquity. *J. Geophys. Res.* 114, E01006. doi:10.1029/2008JE003235

Rae, A. S. P., Collins, G. S., Grieve, R. A. F., Osinski, G. R., and Morgan, J. V. (2017). Complex crater formation: insights from combining observations of shock pressure distribution with numerical models at the West Clearwater Lake impact structure. *Meteorit. Planet. Sci.* 52, 1330–1350. doi:10.1111/maps.12825

Reiff, W. (1977). "The Steinheim Basin – an impact structure," in *Impact and explosion cratering*. Editors D. J. Roddy, R. O. Pepin, R. Merrill, and N. Y. New York (Oxford, United Kingdom: Pergamon Press), 309–320.

Reiff, W. (1979). *Guidebook to the Steinheim Basin impact crater*. Stuttgart, Germany: Geologisches Landesamt Baden-Württemberg, 32.

Reimold, W. U., and Gibson, R. L. (2010). *Meteorite impact! Danger from Space and South Africa's Mega-Impact, the Vredefort Structure*. Berlin, Germany: Springer Publishers, 337.

Reimold, W. U., and Koeberl, C. (2014). Impact structures in Africa – a review. *J. Afr. Earth Sci.* 93, 57–175. doi:10.1016/j.jafrearsci.2014.01.008

Reimold, W. U., Koeberl, C., Gibson, R. L., and Dressler, B. O. (2005). "Economic mineral deposits in impact structures: A review," in *Impact tectonics. Impact studies series*. Editors C. Koeberl, and H. Henkel (Berlin, Germany: Springer-Verlag), 479–552.

Reimold, W. U., Hoffmann, M., Schmitt, R. T., Hauser, N., Zaag, P. T., and Mohr-Westheide, T. (2016). A geochemical contribution to the discussion about the genesis of impact-related pseudotachylitic breccias: studies of PTB in the otavi and kudu quarries of the vredefort dome support the "*in situ* formation" hypothesis. *S. Afr. J. Geol.* 119 (3), 453–472. doi:10.2113/gssajg.119.3.453

Reimold, W. U., Hauser, N., Hansen, B. T., Thirlwall, M., and Hoffmann, M. (2017). The impact pseudotachylitic breccia controversy: insights from first isotope analysis of Vredefort impact-generated melt rocks. *Geochim. Cosmochim. Acta* 214, 266–281. doi:10.1016/j.gca.2017.07.040

Reimold, W. U., Schulz, T., Koenig, S., Koeberl, C., Hauser, N., Wannek, D., et al. (2021). "Genesis of the mafic granophyre of the Vredefort impact structure (South Africa): implications of new geochemical and Se and Re-Os isotopes," in *Large Meteorite Impacts and Planetary Evolution VI*. Editors W. U. Reimold, and C. Koeberl (Boulder, Colorado, United States: Geological Society of America), 235–254. doi:10.1130/2021.2550(09)

Reimold, W. U., Hauser, N., Lopes Oliveira, A., Pereira Maciel, A. R., Goderis, S., Pttarello, L., et al. (2023). Genesis of the mafic impact melt rock in the northwest sector of the Vredefort Dome, South Africa. *Meteorit. Planet. Sci.* 58, 907–944. doi:10.1111/maps.14027

Sahoui, R., Belhai, D., and Jambon, A. (2016). Impact-generated carbonate melts in the Talemzane impact structure (Laghouat, Algeria). *Arab. J. Geosci.* 9, 641. doi:10.1007/s12517-016-2665-6

Sauro, F., Payler, S. J., Massironi, M., Pozzobon, R., Hiesinger, H., Mangold, N., et al. (2023). Training astronauts for scientific exploration on planetary surfaces: the ESA PANGAEA programme. *Acta Astronaut.* 204, 222–238. doi:10.1016/j.actaastro.2022.12.034

Schmieder, M., and Kring, D. A. (2020). Earth's impact events through geologic time: A list of recommended ages for terrestrial impact structures and deposits. *Astrobiology* 20 (1), 91–141. doi:10.1089/ast.2019.2085

Schmieder, M., Schwarz, W. H., Trieloff, M., Tohver, E., Buchner, E., Hopp, J., et al. (2015). New ^{40}Ar-^{39}Ar dating of the Clearwater Lake impact structures (Québec, Canada) – not the binary asteroid impact it seems? *Geochim. Cosmochim. Acta* 148, 304–324. doi:10.1016/j.gca.2014.09.037

Schmieder, M., Sach, V. J., and Buchner, E. (2022). The Chöpfi pinnacles near Winterthur, Switzerland: long distance effects of the Ries impact earthquake? *Int. J. Earth Sci.* 111, 145–147. doi:10.1007/s00531-021-02082-0

Shand, R. J. (1916). The pseudotachylyte of Parijs (Orange Free State) and its relation to "trap-shotten gneiss" and 'flinty crush-rock. *Quart. J. Geol. Soc. Lond.* 72, 198–221. doi:10.1144/gsl.jgs.1916.072.01-04.12

Shoemaker, E. M., and Chao, E. C. T. (1961). New evidence for the impact origin of the Ries basin, Bavaria, Germany. *J. Geophys. Res.* 66, 3371–3378. doi:10.1029/JZ066i010p03371

Simpson, S. L., Osinski, G. R., Longstaffe, F. R., Schmieder, M., and Kring, D. A. (2020). Hydrothermal alteration associated with the Chicxulub impact crater upper peak-ring breccias. *Earth Planet. Sci. Lett.* 547, 116425. doi:10.1016/j.epsl.2020.116425

Stöffler, D., and Grieve, R. A. F. (2007). "Impactites," in *Metamorphic rocks: A classification and glossary of terms. Recommendations of the international subcommission on the systematics of metamorphic rocks*. Editors D. Fettes, and J. Desmons (Cambridge, UK: Cambridge University Press), 82–92.

Stöffler, D., Artemieva, N. A., Wünnemann, K., Reimold, W. U., Jacob, J., Hansen, B. K., et al. (2013). Ries crater and suevite revisited – observations and modeling Part I.: observations. *Meteorit. Planet. Sci.* 48, 515–589. doi:10.1111/maps.12086

Stöffler, D., Hamann, C., and Metzler, K. (2018). Shock metamorphism of planetary silicate rocks and sediments: proposal for an updated classification system. *Meteorit. Planet. Sci.* 53, 5–49. doi:10.1111/maps.12912

Stöffler, D., Hamann, C., and Metzler, K. (2019). Shock metamorphism of planetary silicate rocks and sediments: proposal for an updated classification system. *Meteorit. Planet. Sci.* 53, 946–949. doi:10.1111/maps.13246

Therriault, A. M. (1992). *Field study, petrology, and chemistry of the Vredefort Granophyre, South Africa*. M.Sc. Dissertation. Houston, Tx, USA: Univ. of Houston, 347.

Therriault, A. M., Fowler, A. D., and Grieve, R. A. F. (2002). The Sudbury igneous complex? A differentiated impact melt sheet. *Econ. Geol.* 97, 1521–1540. doi:10.2113/gsecongeo.97.7.1521

Tohver, E., Cawood, P. A., Riccomini, C., and Trindade, R. I. F. (2013). Shaking a methane fizz: seismicity from the araguainha impact event and the permian-triassic global carbon isotope record. *Palaeogeogr, Palaeoclim. Palaeoecol.* 387, 66–75. doi:10.1016/j.palaeo.2013.07.010

Tolometti, G. D., Erickson, T. M., Osinski, G. R., Vayron, C., and Neish, C. D. (2022). Hot rocks: constraining the thermal conditions of the Mistastin Lake impact melt deposits using zircon grain microstructures. *Earth Planet. Sci. Lett.* 584, 117523. doi:10.1016/j.epsl.2022.117523